Chapter 4

Result and Discussion

4.1 Characteristics of starting materials

4.1.1 The thermal transformation

The DTA/TG curves of the starting materials indicated the thermal transformation and % weight loss, as illustrated in Figures 4-1, 4-2, and 4-3.

From the DTA curve, it was found that the endothermic peak of the loss of water occurred at about 100 ^{o}C, the endothermic peak of dehydration occurred at about 300 ^{o}C, the exothermic peak of phase change occurred at about 400 ^{o}- 500 ^{o}C, and the endothermic peak of melting occurred at about 980 ^{o}C. The exothermic peak of phase change at about 400 ^{o}- 500 ^{o}C could be confirmed by XRD patterns which shown phase change at above 350 ^{o}C (see 4.1.2).

Two endothermic peaks of dehydration of CP2 and CP3 were observed. It could be explained that there was the dehydration of two components in the starting materials. While it was also found two phases of starting materials in XRD patterns. (see 4.1.2) In case of CP1, it had less amount of a trace component until DTA curve showed only one endothermic peak of dehydration.

Moreover, the TG curve showed % weight loss which occurred at about 250 °- 500 °C in dehydration segment. Therefore, DTA/TG and XRD supported the results that $Ca(H_2PO_4)_2$ and $CaHPO_4$ lost the intramolecular water and changed to be new phases, i.e., $Ca(PO_3)_2$ and $Ca_2P_2O_7$.(XRD patterns were shown in Figures 4-6, 4-7, and 4-8.)

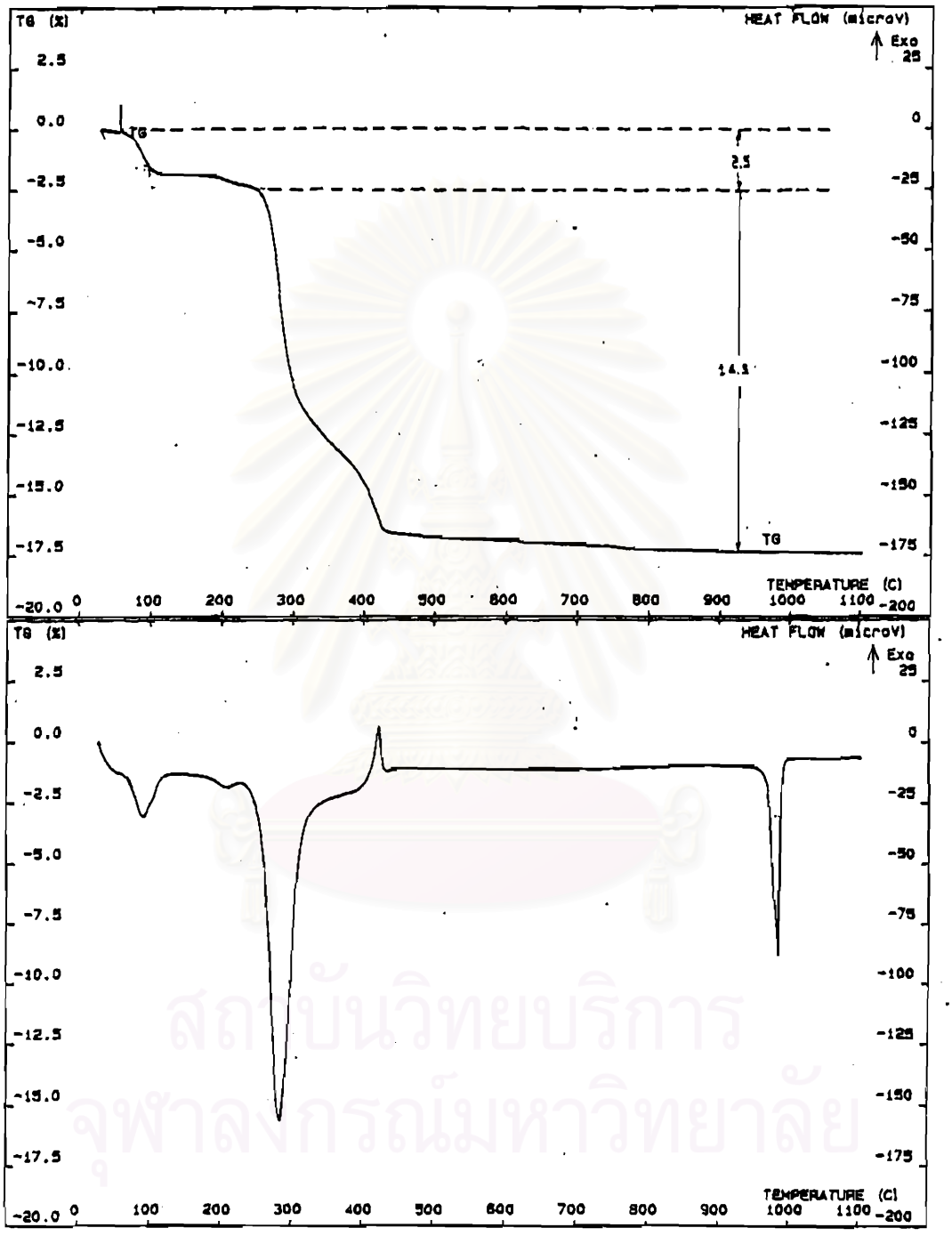

Figure 4-1 DTA/TG curves of CP1 starting material.

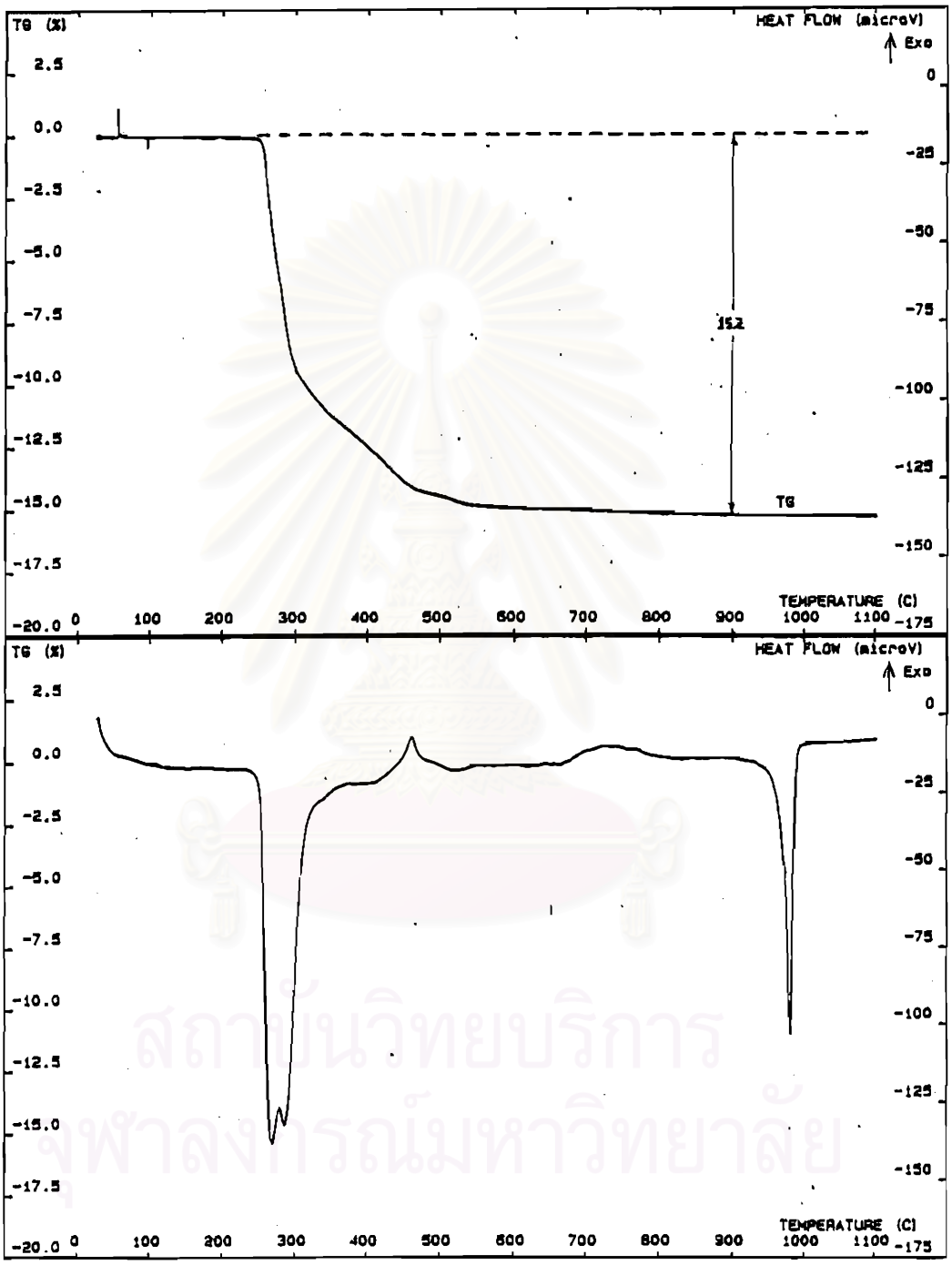

Figure 4-2 DTA/TG curves of CP2 starting material.

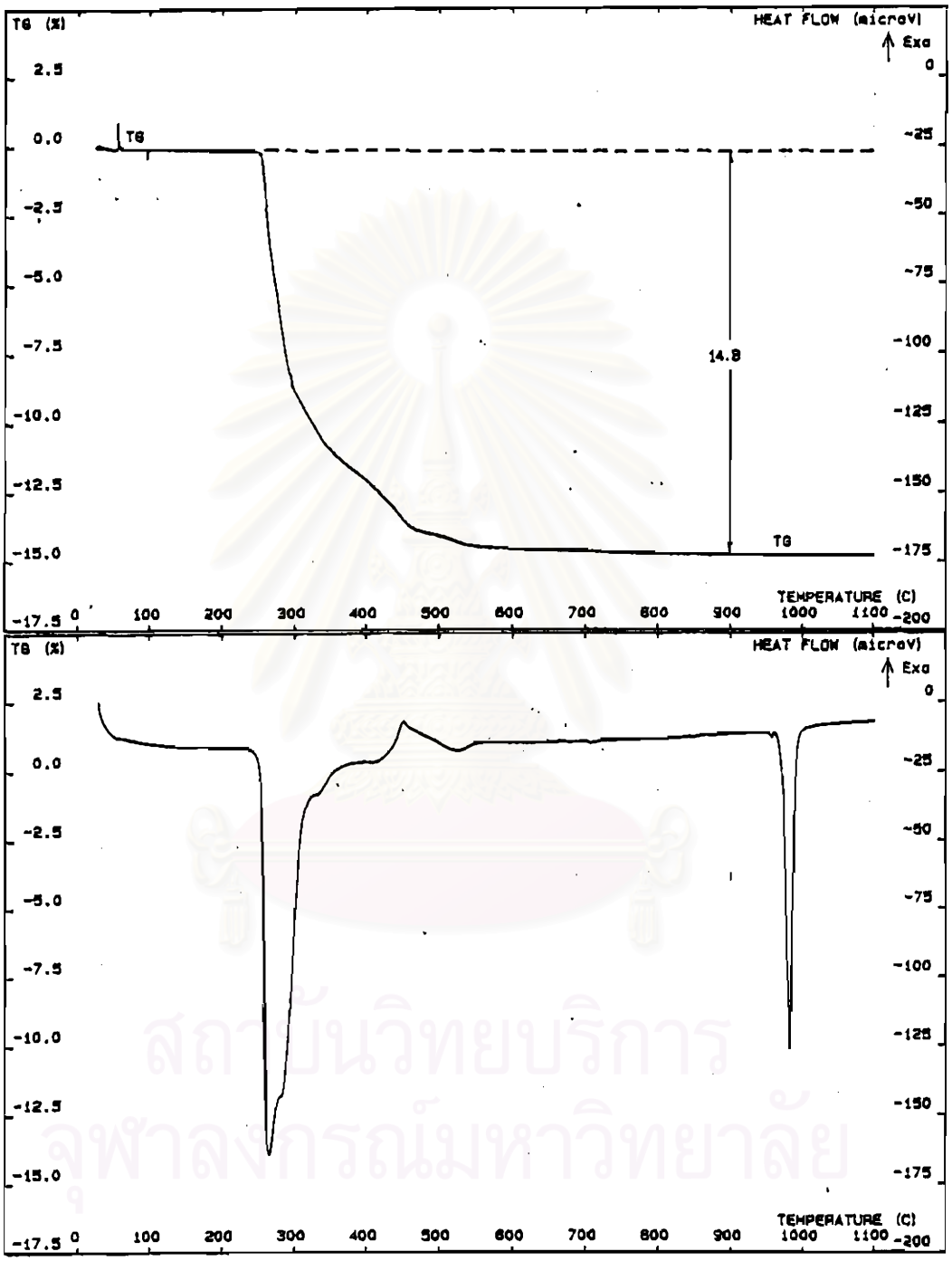

Figure 4-3 DTA/TG curves of CP3 starting material.

4.1.2 Phase present of starting material

For preparation of starting material, the reaction of calcium carbonate ($CaCO_3$) with orthophosphoric acid (H_3PO_4) gives two phases: calcium monohydrogen phosphate ($CaHPO_4$) and calcium dihydrogen phosphate [$Ca(H_2PO_4)_2$]. From XRD patterns, it was found that $Ca(H_2PO_4)_2$ was the main phase and there was a trace of $CaHPO_4$. At high temperature, there was a phase change of $Ca(H_2PO_4)_2$ and $CaHPO_4$. At 350 ^{0}C, $Ca(H_2PO_4)_2$ changed to γ-calcium metaphosphate [γ-$Ca(PO_3)_2$] and β-calcium metaphosphate [β-$Ca(PO_3)_2$] as a main phase and $CaHPO_4$ changed to β-calcium diphosphate (β-$Ca_2P_2O_7$). At 550 ^{o}C, there was the phase transformation of γ-calcium metaphosphate [γ-$Ca(PO_3)_2$] to β-calcium diphosphate (β-$Ca_2P_2O_7$); it was found that the decreasing of γ-$Ca(PO_3)_2$ with the increase of β-$Ca(PO_3)_2$. At 750 ^{o}C, the phases present were only β-$Ca(PO_3)_2$ and β-$Ca_2P_2O_7$. The change of the starting materials at different temperatures were illustrated in Figure 4-4 and Table 4-1.

Table 4-1 The occurrence of phase at different temperatures

Temperature	Phase
Room temperature	$Ca(H_2PO_4)_2$, $CaHPO_4$
350 ^{o}C	γ-$Ca(PO_3)_2$, β-$Ca(PO_3)_2$, β-$Ca_2P_2O_7$
550 ^{o}C	β-$Ca(PO_3)_2$, β-$Ca_2P_2O_7$
750 ^{o}C	β-$Ca(PO_3)_2$, β-$Ca_2P_2O_7$

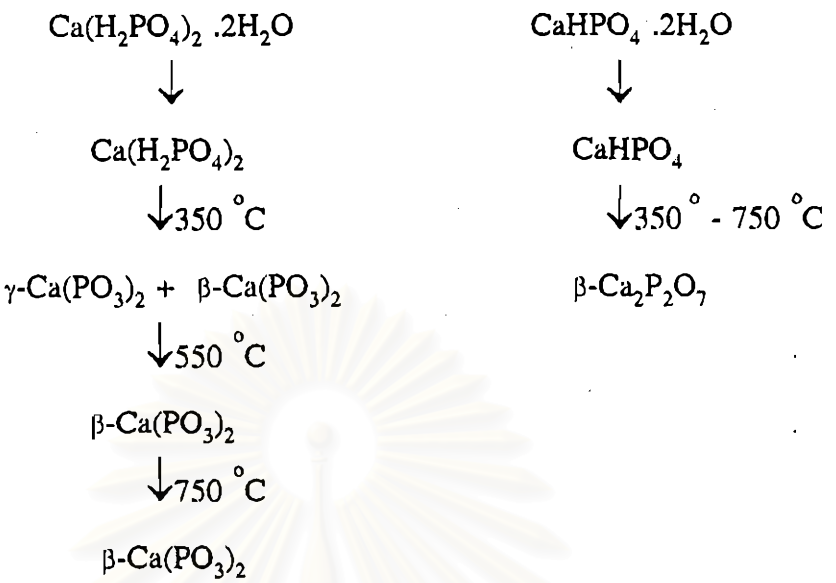

Figure 4-4 Flow chart of the phase transformation of the starting material components.

The phase transformation of starting material components was in agreement with the phase transformation of $Ca(H_2PO_4)_2 \cdot 2H_2O$ and $CaHPO_4 \cdot 2H_2O$ which was expressed by Aoki[36] as shown in Figure 4-5.

The XRD patterns of CP1, CP2, and CP3 starting materials at room temperature, 350 °C, 550 °C, 750 °C were illustrated in Figure 4-6, 4-7 and 4-8, respectively. (The reference of XRD patterns of $Ca(H_2PO_4)_2$ and $CaHPO_4$ at room temperature, 350 °C, and 750 °C were illustrated in Appendices B and C.)

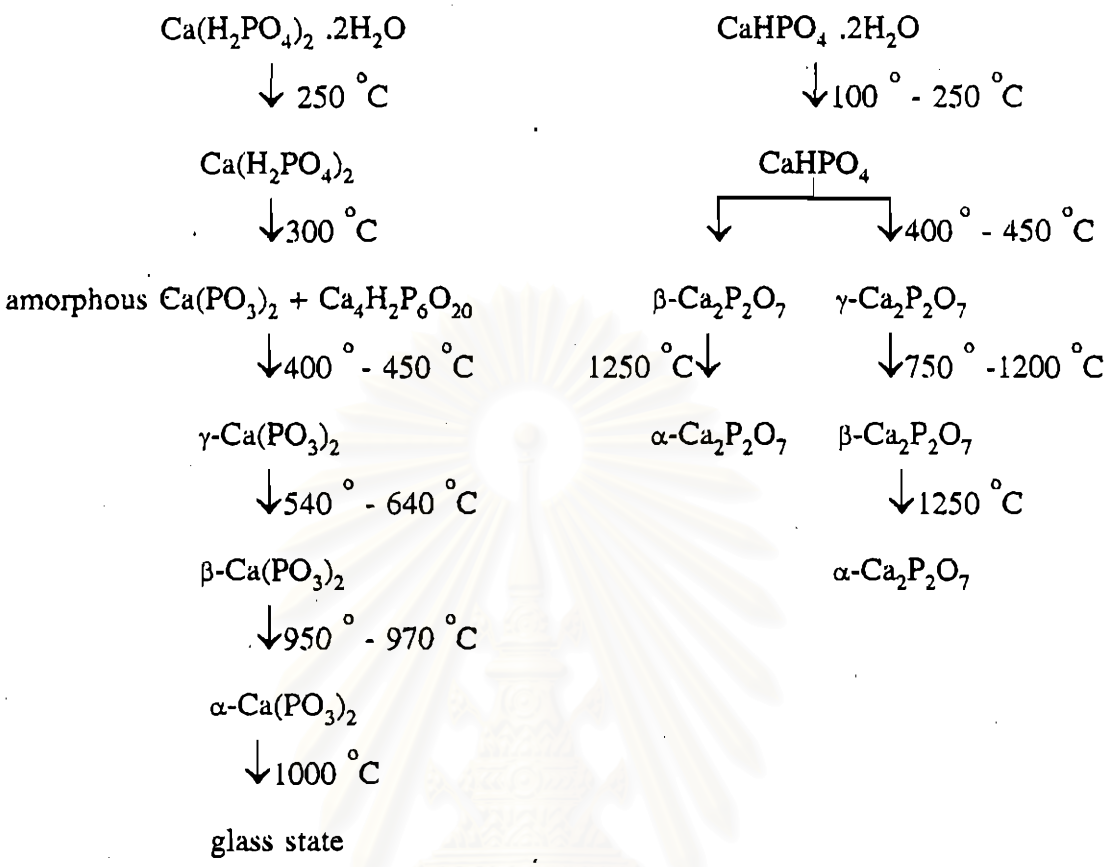

Figure 4-5 The phase transformation of $Ca(H_2PO_4)_2 \cdot 2H_2O$ and $CaHPO_4 \cdot 2H_2O$ [36]

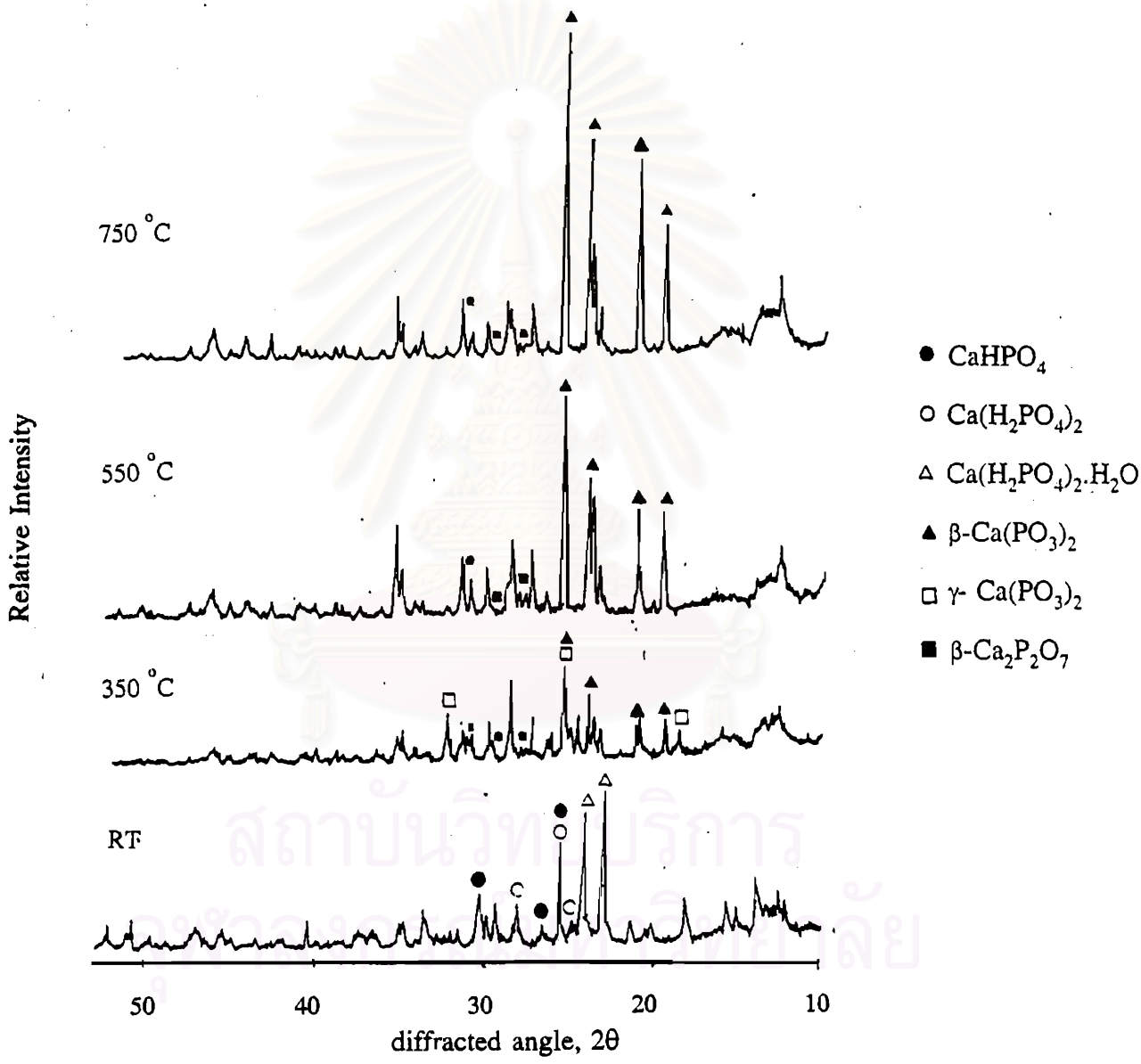

Figure 4-6 XRD patterns of CP1 starting material at room temperature, 350°C, 550°C, and 750°C.

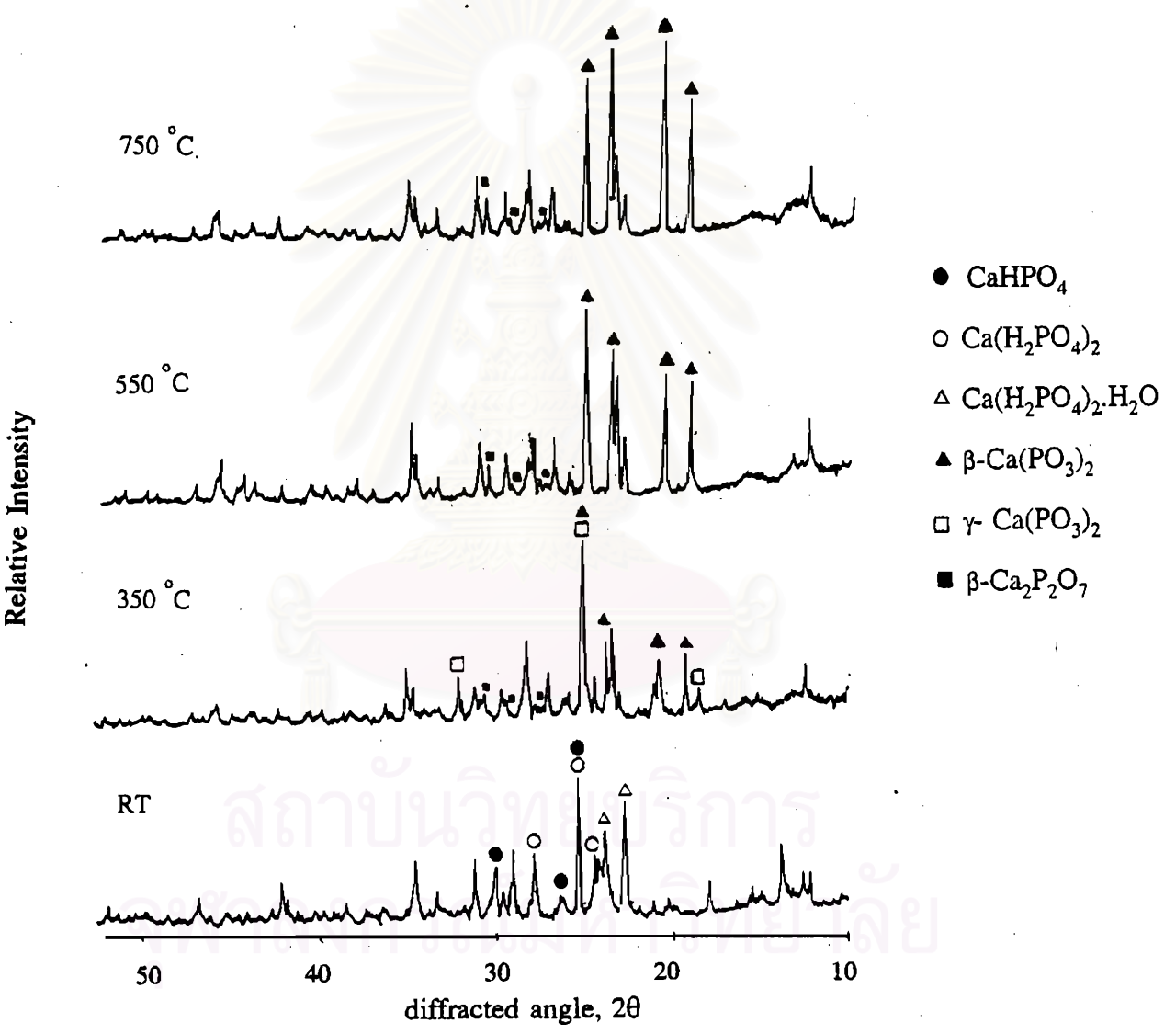

Figure 4-7 XRD patterns of CP2 starting material at room temperature, 350°C, 550°C, and 750°C.

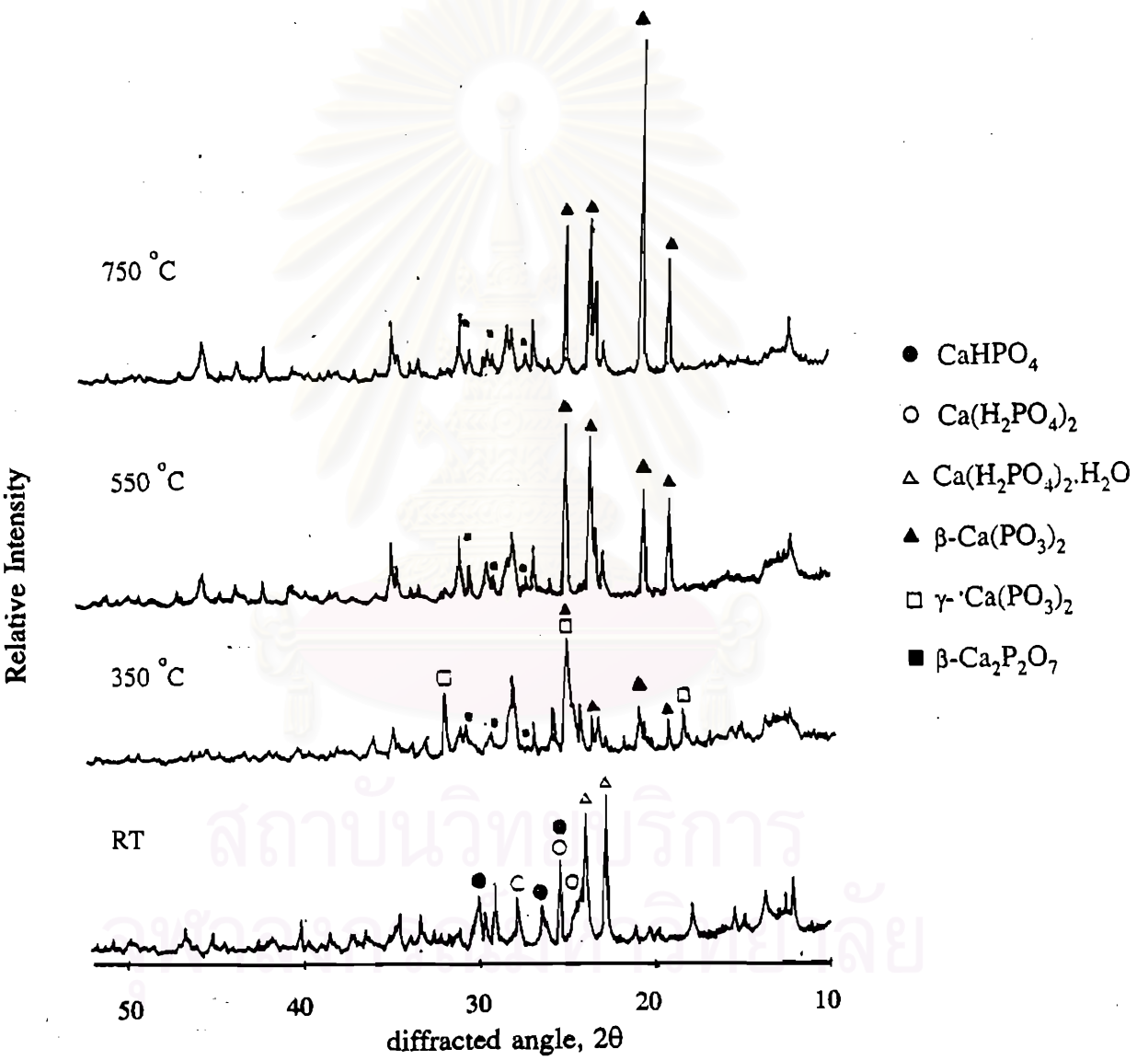

Figure 4-8 XRD patterns of CP3 starting material at room temperature, 350°C, 550°C, and 750°C.

4.1.3 Functional groups of starting material

The functional groups of starting materials indicated: ν OH at about 3500 cm^{-1}, ν_{as} PO_2 at about 1250 cm^{-1}, ν PO_2 at about 1095 cm^{-1}, ν_{as} POP at about 890 cm^{-1}, ν POP at about 770 and 720 cm^{-1}, and δ PO at about 530 and 480 cm^{-1}. At room temperature condition, it was found the water peak appeared in FT-IR spectra; and it disappeared at higher temperature because of the loss of water. OH group found in FT-IR spectra, indicated the presence of the bonding between H-atom and O-atom of PO_4 chain structure. And this bonding led to the stop of the phosphate chain at the terminal structure.

The FT-IR spectra of CP1, CP2, and CP3 starting materials were illustrated in Figure 4-9, 4-10, and 4-11.

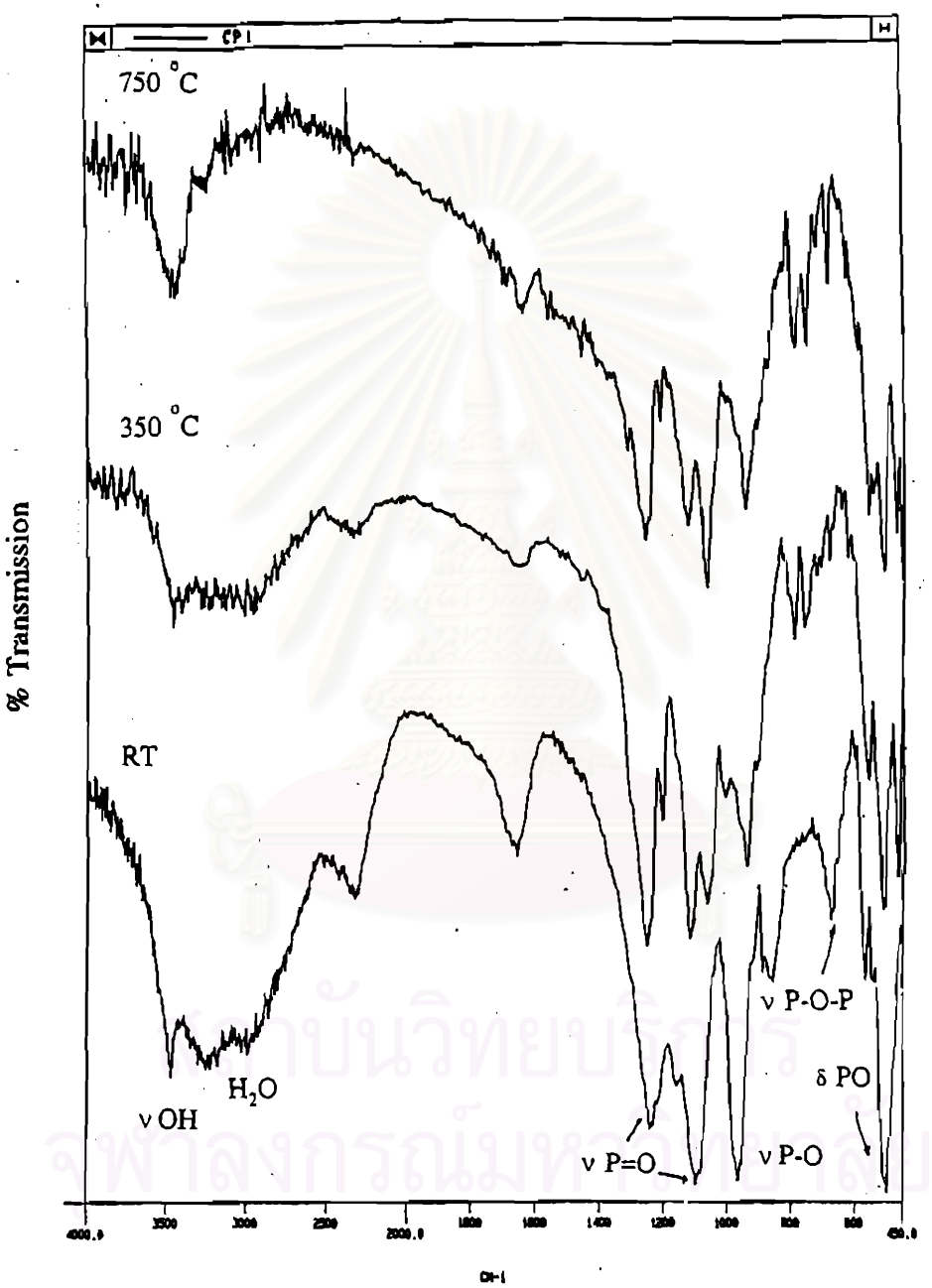

Figure 4-9 FT-IR spectra of CP1 starting material.

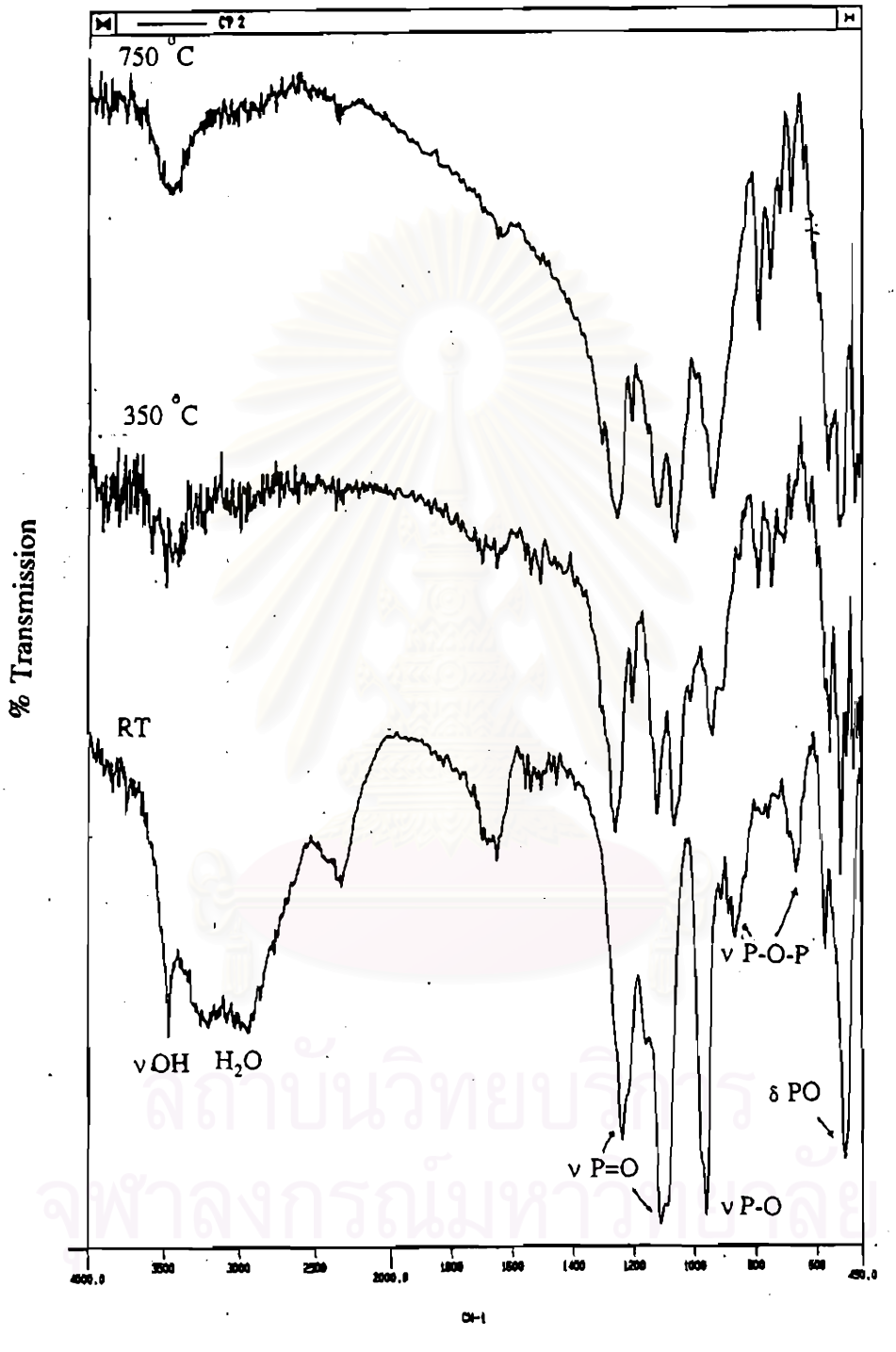

Figure 4-10 FT-IR spectra of CP2 starting material.

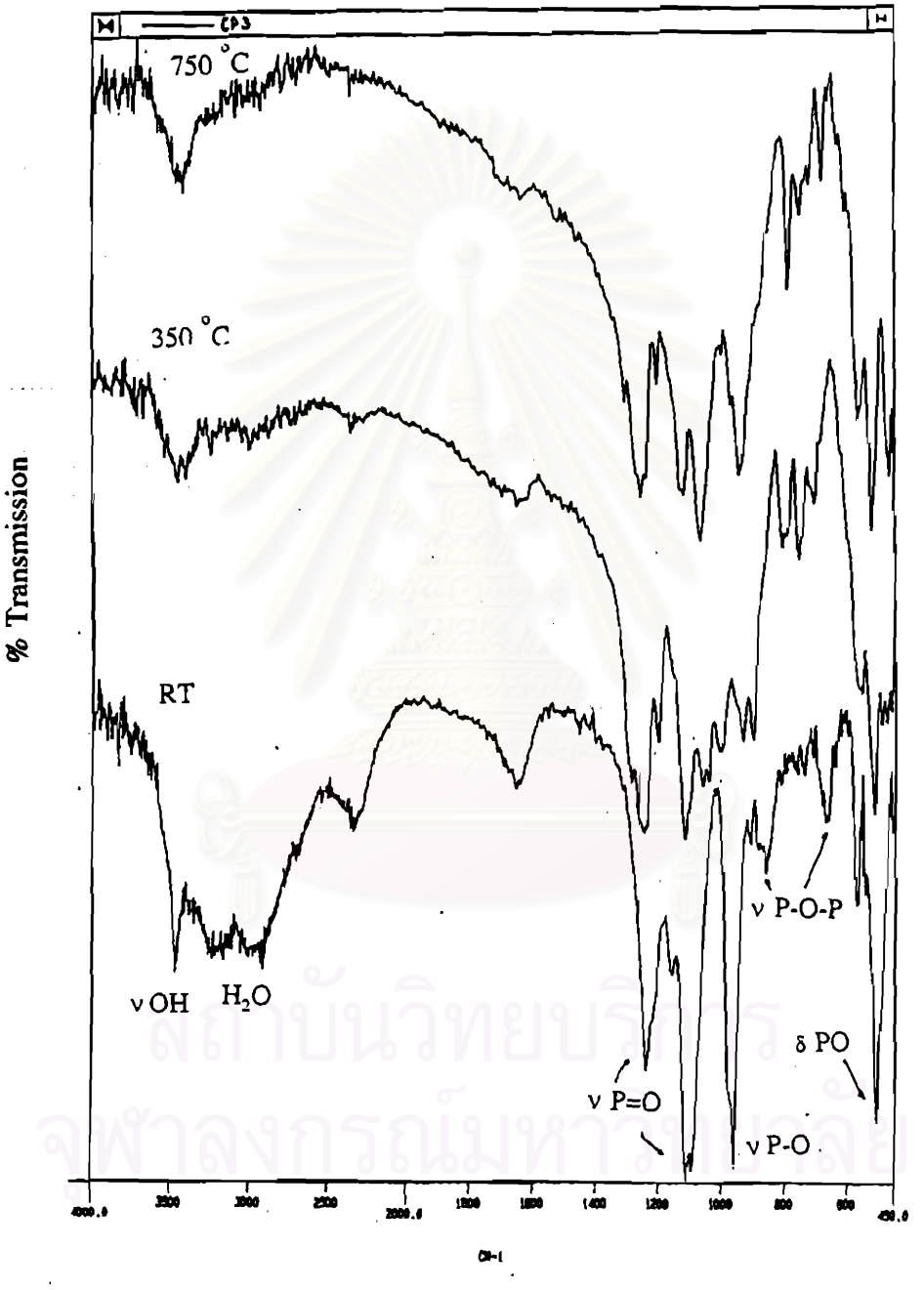

Figure 4-11 FT-IR spectra of CP3 starting material.

4.2 Characteristics of glass samples

4.2.1 Chemical composition of glass samples

The CPG, CPG1, CPG2, and CPG3 glass samples were analyzed, as illustrated in Tables 4-2 and 4-3.

Table 4-2 Chemical composition of glass samples by wet chemical analysis.

Glass sample	CaO (mol %)[1]	P_2O_5 (mol %)[2]
CPG	49.98	49.90
CPG1	49.96	49.95
CPG2	51.26	49.14
CPG3	52.13	49.11

[1] Analysis by the precipitate of CaC_2O_4 [2] Analysis by molybdovanadate method

Table 4-3 Chemical composition of glass sample by XRF borate fusion method*

Glass	SiO_2	Al_2O_3	Fe_2O_3	MgO	CaO	Na_2O	K_2O	TiO_2	P_2O_5	MnO	Cr_2O_3
CPG	0.01	0.06	<0.006	0.15	50.46	<0.08	<0.01	0.01	49.81	<0.01	0.04
CPG1	3.76	2.18	0.06	<0.12	48.86	0.08	0.09	0.06	47.41	<0.01	0.006
CPG2	2.71	1.66	0.04	0.37	50.82	0.08	0.03	0.04	47.55	<0.01	0.01
CPG3	0.92	0.59	0.02	0.32	54.03	0.08	0.02	0.02	47.62	<0.01	0.01

* These results were analyzed by Mineral Assays and Service Co.,Ltd. , Canada .

From the chemical analysis by XRF borate fusion method, the increasing impurities occurred from the corrosion between the molten glass and the crucible. And it was found that the corrosion increase depended on the amount of P_2O_5. In this experiment, the corrosion of glass samples increased in the following order, CPG1 > CPG2 > CPG3 .

4.2.2 Functional groups of starting materials

The functional groups of glass samples indicated: ν OH at about 3500 cm^{-1}, ν_{as} PO_2 at about 1250 cm^{-1}, ν PO_2 at about 1095 cm^{-1}, ν_{as} POP at about 890 cm^{-1}, ν POP at about 770 and 720 cm^{-1}, and δ PO at about 530 and 480 cm^{-1}. Similar to 4.1.3, OH group led to stop the chain of phosphate glass at the terminal.

The FT-IR spectra of CPG, CPG1, CP2, and CP3 glass samples were illustrated in Figure 4-12.

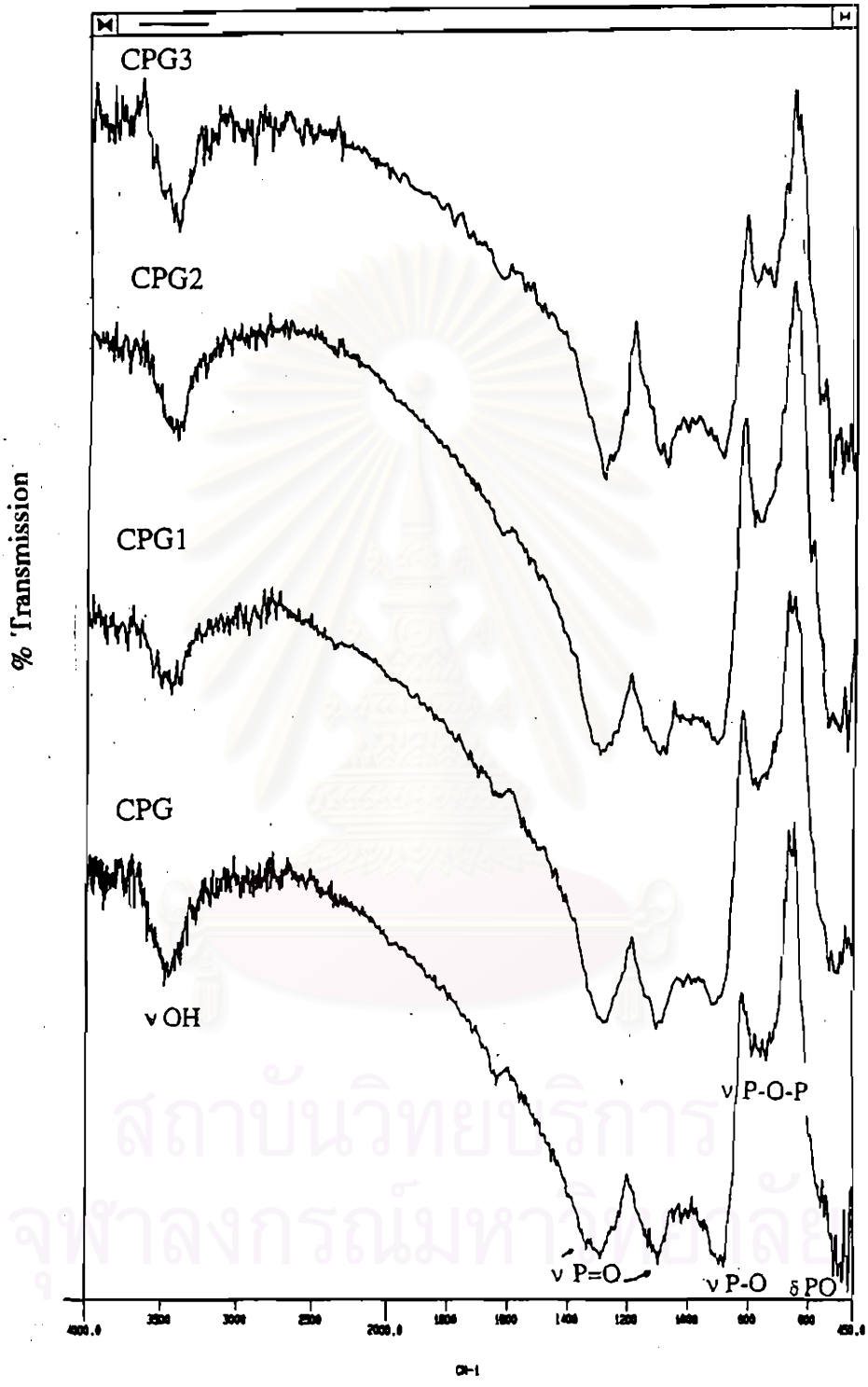

Figure 4-12 FT-IR spectra of CPG, CPG1, CPG2, and CPG3 glass samples.

4.2.3 Thermal expansion

The thermal expansion curves of CPG, CPG1, CPG2, and CPG3 glass samples were illustrated in Figure 4-13.

From the thermal expansion curves, it indicated two points: the transition temperature (T_g) and the softening temperature (T_{soft}). These data were illustrated in Table 4-4.

Table 4-4 Illustration of T_g and T_{soft} of glass sample

Glass sample	T_g °C	T_{soft} °C
CPG	507	562
CPG1	504	549
CPG2	514	553
CPG3	517	566

The comparison between CPG and CPG1 which contained $CaO:P_2O_5$ = 50:50 mol% as the same. CPG1 contained with high impurities would be the lower transition and softening temperatures than CPG. This could be shown that the contaminated impurities changed the behavior of glass.

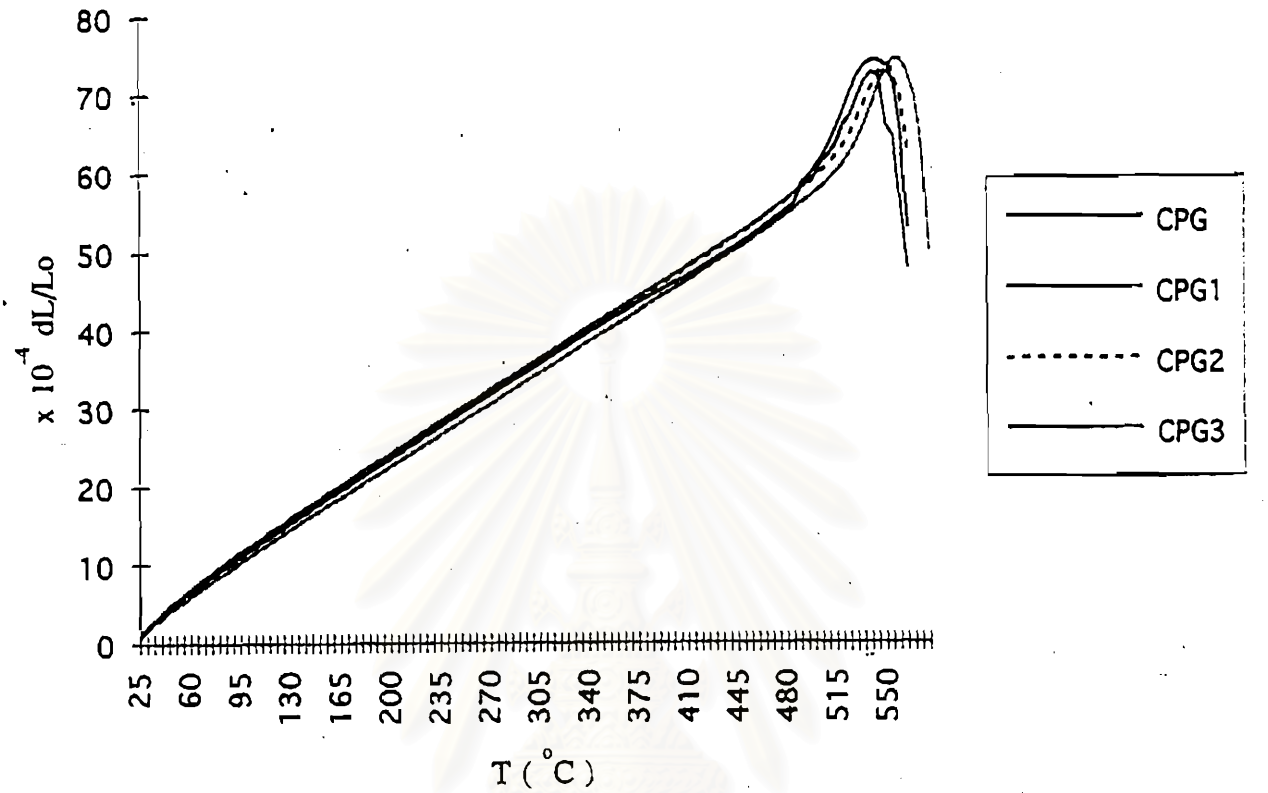

Figure 4-13 Thermal expansion of CPG, CPG1, CPG2, and CPG3 glass samples.

4.2.4 Thermal transformation

The thermal transformation of glass sample was analyzed in Table 4-5 and Figures 4-14, 4-15, 4-16 and 4-17. Whereas DTA curve could indicate three points: transition temperature (T_g), crystallization temperature (T_c), and melting temperature (T_m) of glass.

Table 4-5 The thermal transformations of CPG, CPG1, CPG2, and CPG3 glass samples.

Glass sample	T_g °C	T_c °C	T_m °C
CPG	510	630	983
CPG1	540	682 , 742	937 , 947
CPG2	530	675 , 720	948 , 966
CPG3	540	676	967 , 985

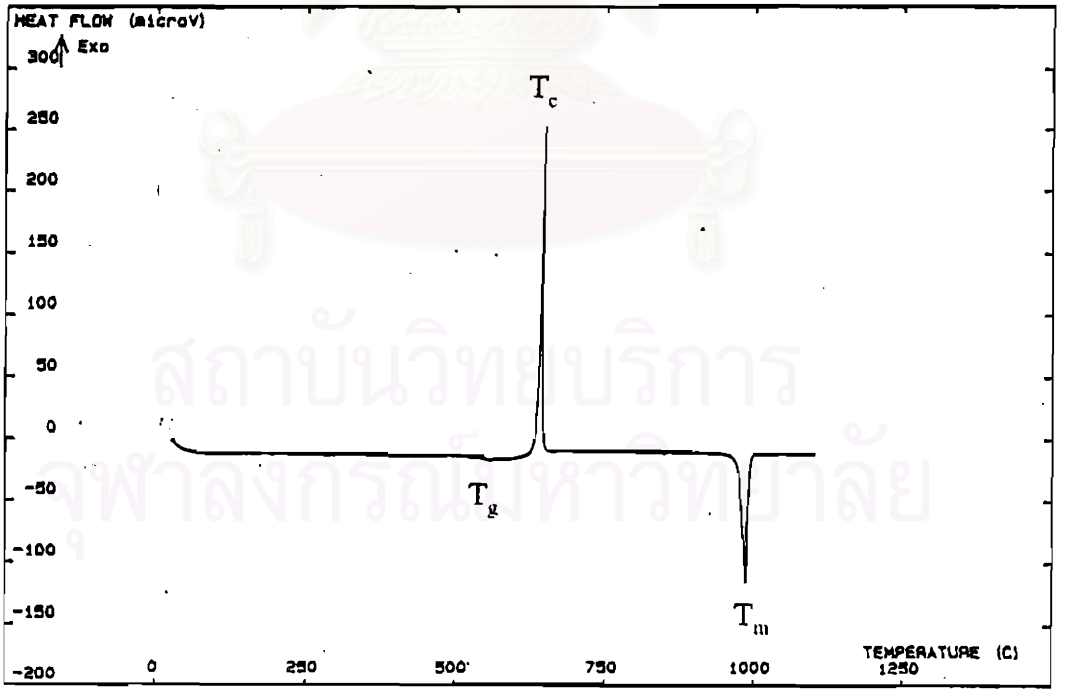

Figure 4-14 DTA curve of CPG glass sample.

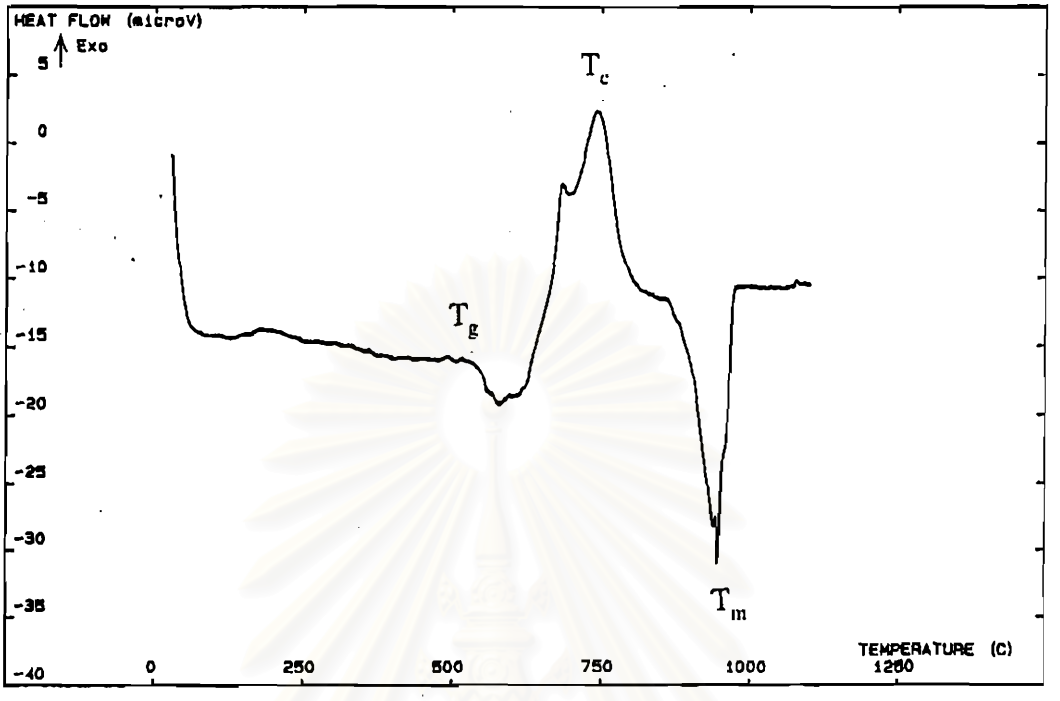

Figure 4-15 DTA curve of CPG1 glass sample.

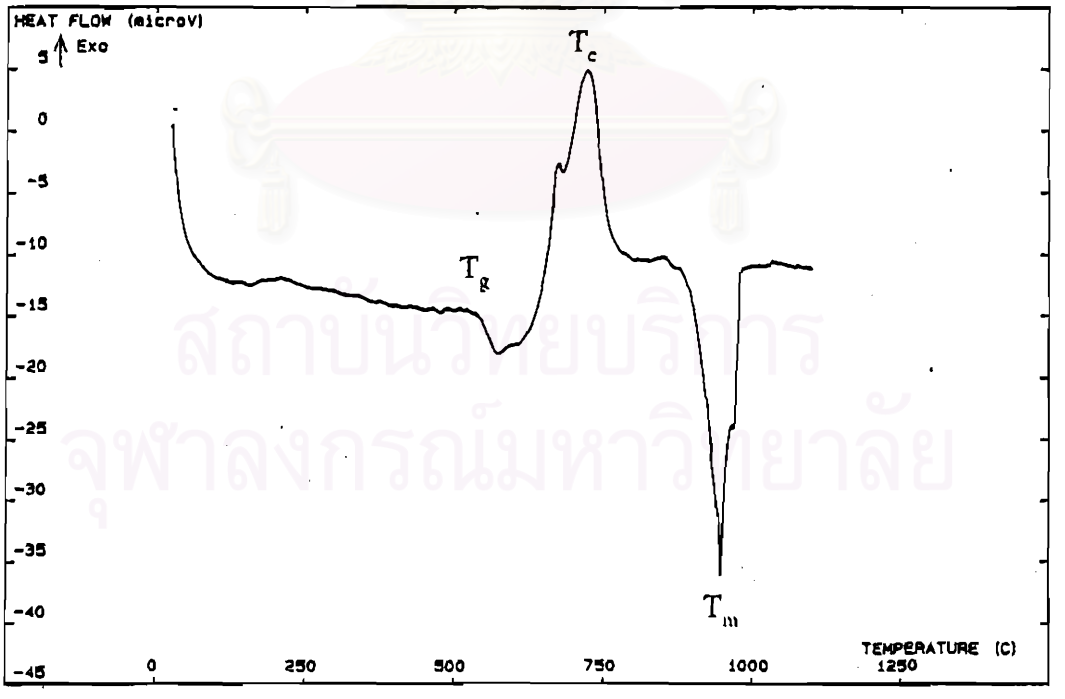

Figure 4-16 DTA curve of CPG2 glass sample.

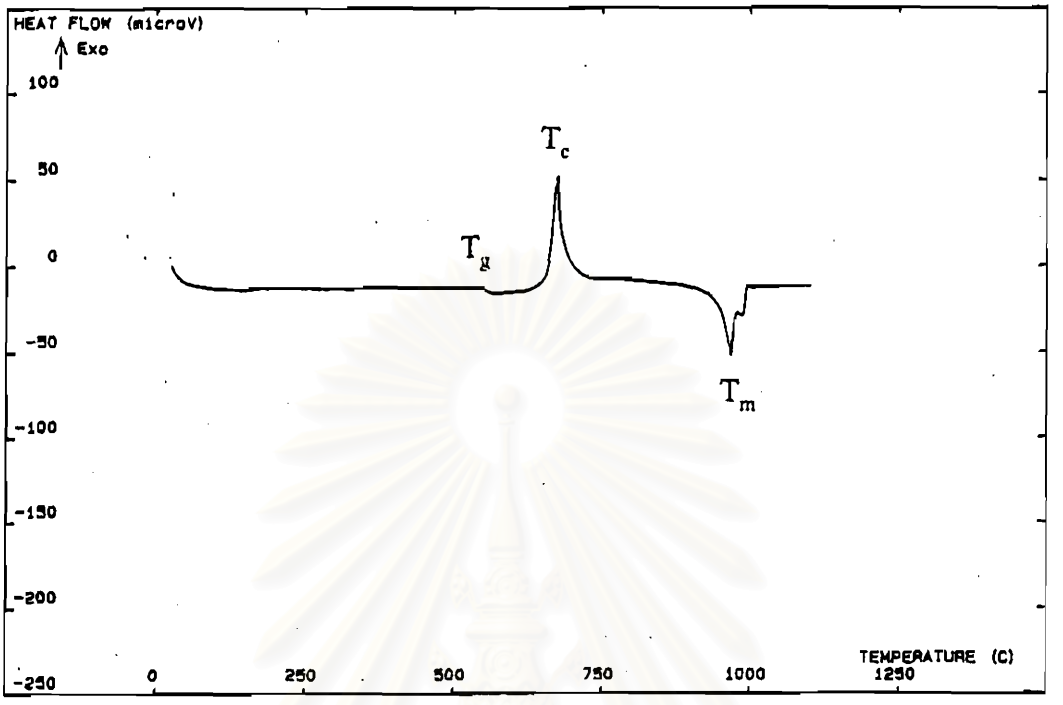

Figure 4-17 DTA curve of CPG3 glass sample.

DTA curve of CPG1 and CPG2 was shown two exothermic peaks of crystallization . The appearance of a small peak was indicated that it was a metaphase of crystallization and it was examined by XRD at different temperatures in 4.3.4.

In addition , DTA curve of CPG1 , CPG2 , and CPG3 was also shown two endothermic peaks of melting. A small peak of melting endothermic peak was an effect of impurities which contaminated in the glass. During the melting, there was a corrosion between a molten glass and a crucible; the components of crucible were leached out as the impurities and bonded with phosphate chain to new components.

4.3 Nucleation and crystallization behavior of glass

4.3.1 Nucleation rate temperature-like curve

The nucleation rate curve of CPG, CPG1, CPG2, and CPG3 glass samples was shown in Figures 4-18, 4-19, 4-20, and 4-21. From this nucleation rate-temperature-like curve, the maximum nucleation temperature was detected. At this maximum nucleation temperature, there was the largest number of nuclei to occur. The maximum nucleation temperature of CPG, CPG1, CPG2, and CPG3 occurred at 487 °, 569 °, 559 °, and 579 °C, respectively.

Table 4-6 Illustration of T_n and T_p of CPG, CPG1, CPG2, and CPG3

CPG		CPG1		CPG		CPG3	
T_n °C	T_p °C	T_n °C	T_p °C	T_n °C	T_p °C	T_n °C	T_p °C
456.4	618.4	559.5	719:1	538.8	695.5	529.1	652.4
466.3	619.6	569.4	715.7	549.1	695.6	539.4	649.9
473.2	613.7	579.6	715.9	554.0	693.8	549.2	647.2
487.0	602.3	589.8	719.5	559.0	690.1	559.2	647.0
496.7	605.0	620.6	719.0	564.4	695.1	569.4	643.9
506.8	607.2			579.0	695.0	579.3	635.4
						589.5	653.3
						600.0	667.1

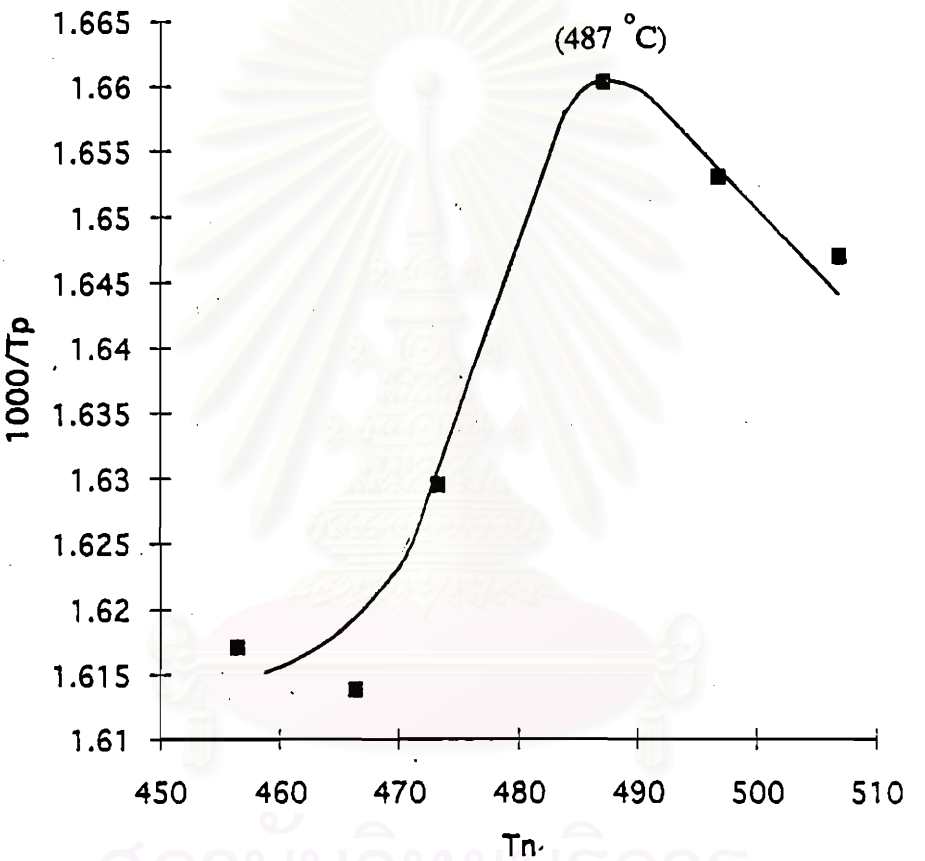

Figure 4-18 The nucleation rate-temperature-like curve of CPG glass sample.

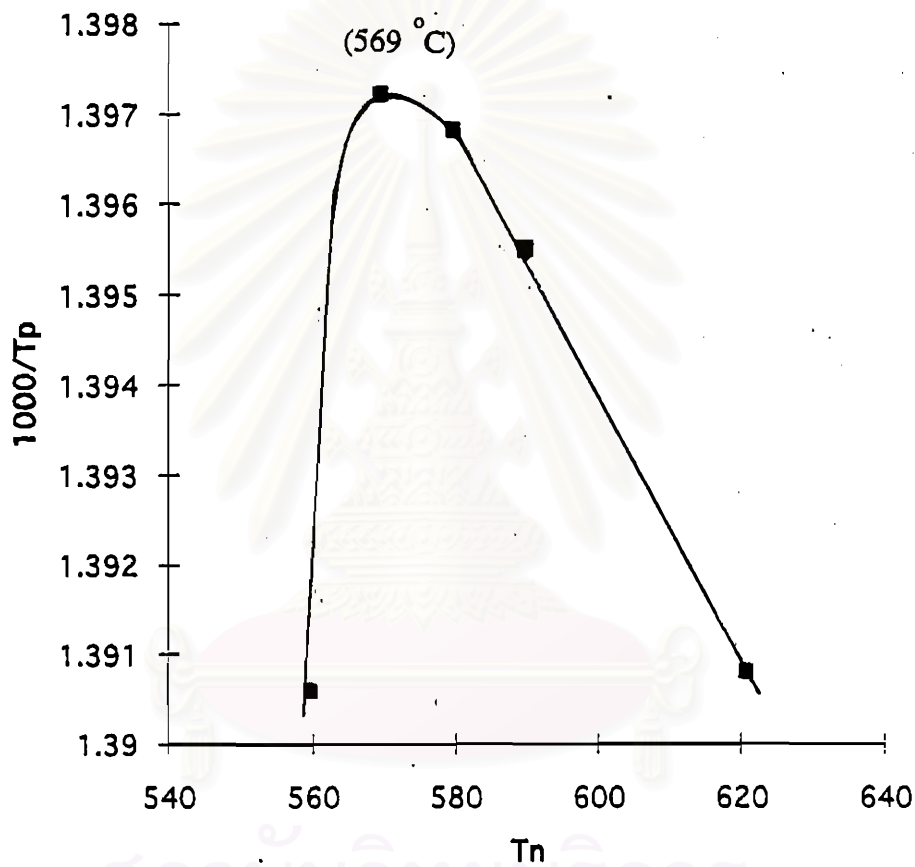

Figure 4-19 The nucleation rate-temperature-like curve of CPG1 glass sample.

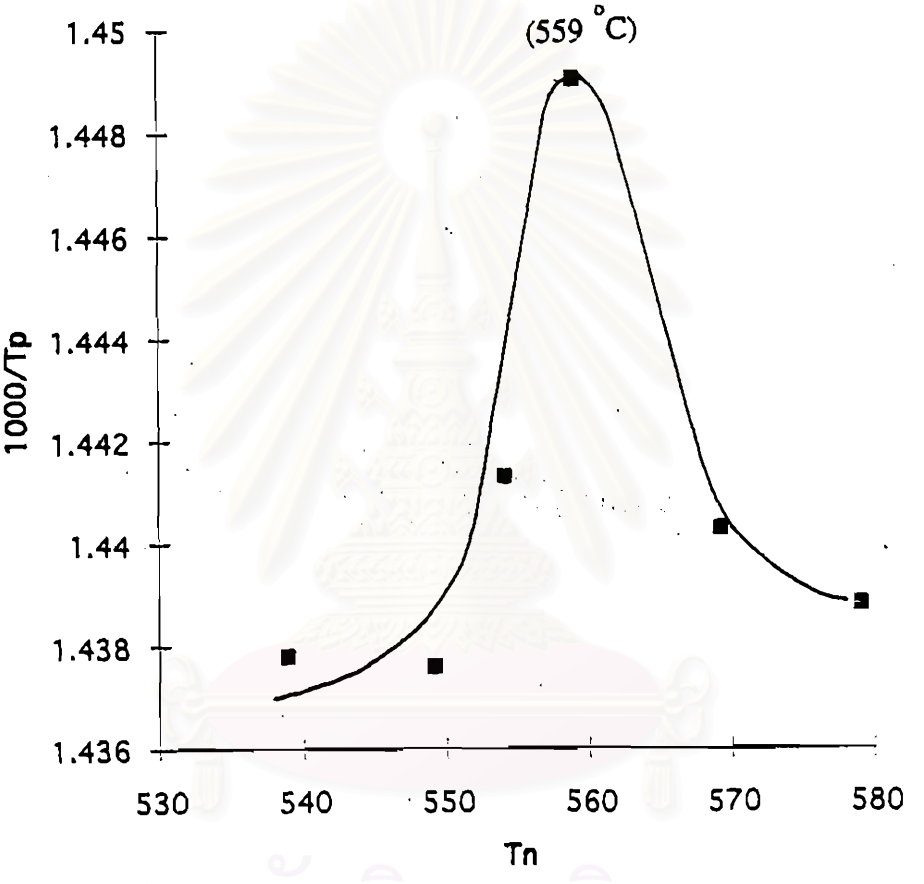

Figure 4-20 The nucleation rate-temperature-like curve of CPG2 glass sample.

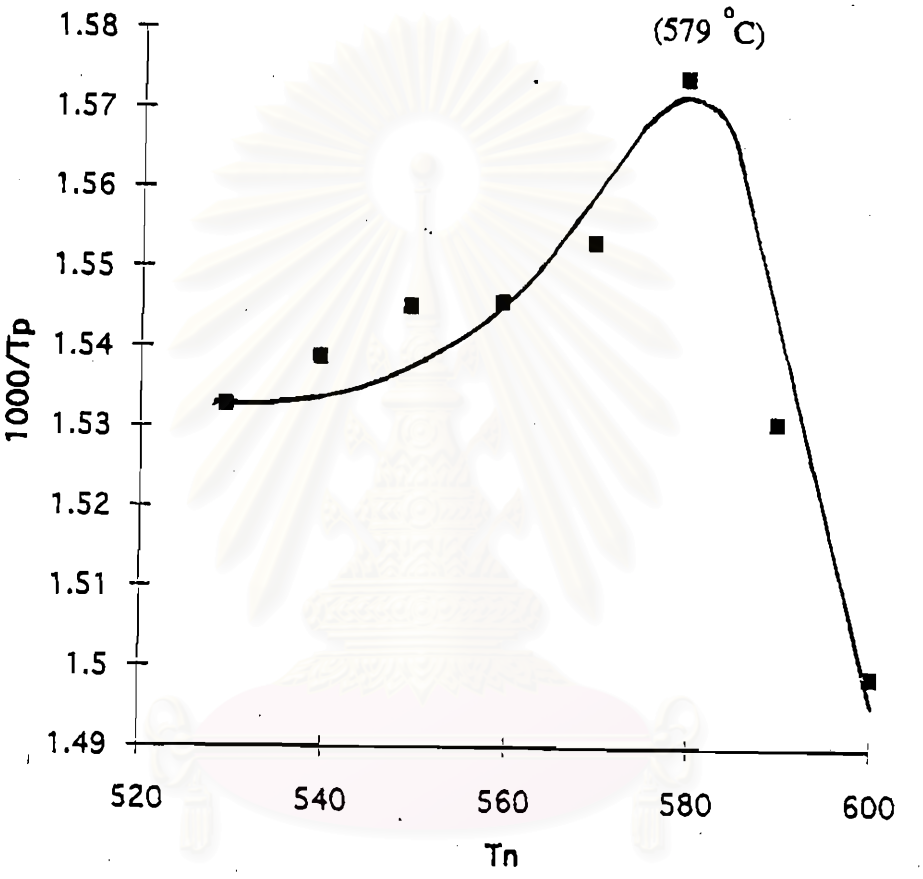

Figure 4-21 The nucleation rate-temperature-like curve of CPG3 glass sample.

4.3.2 The kinetics of crystallization

In the nonisothermal method, the activation energy of crystallization (E) and Avrami parameter (n) were used to explained the behavior of glass. These values were illustration in Table 4-7.

Table 4-7 The activation energy of crystallization and Avrami parameter of glass samples.

Glass sample	E (kJ/mol)	n
CPG	117.9	29.0
CPG1	363.3	0.94
CPG2	236.8	1.50
CPG3	244.3	4.00

Table 4-8 Illustration of T_p at different heating rates of CPG, CPG1, CPG2, and CPG3.

heating rate	T_p °C CPG	T_p °C CPG1	T_p °C CPG2	T_p °C CPG3
5	628.6	723.5	699.9	657.5
8	641.5	724.9	707.8	663.3
10	647.7	730.2	713.0	666.7
12	651.0	730.9	714.3	-
15	658.3	735.1	718.0	673.2

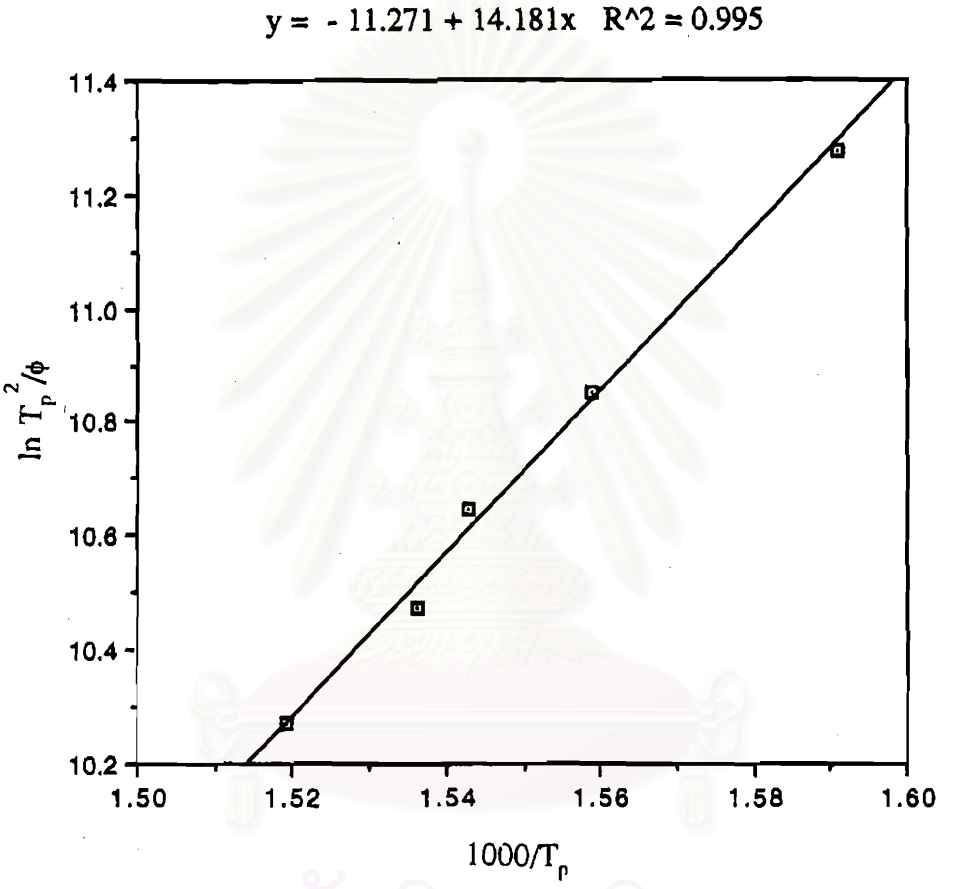

Figure 4-22 Plot of ln T_p^2/ϕ and $1000/T_p$ of CPG glass sample.

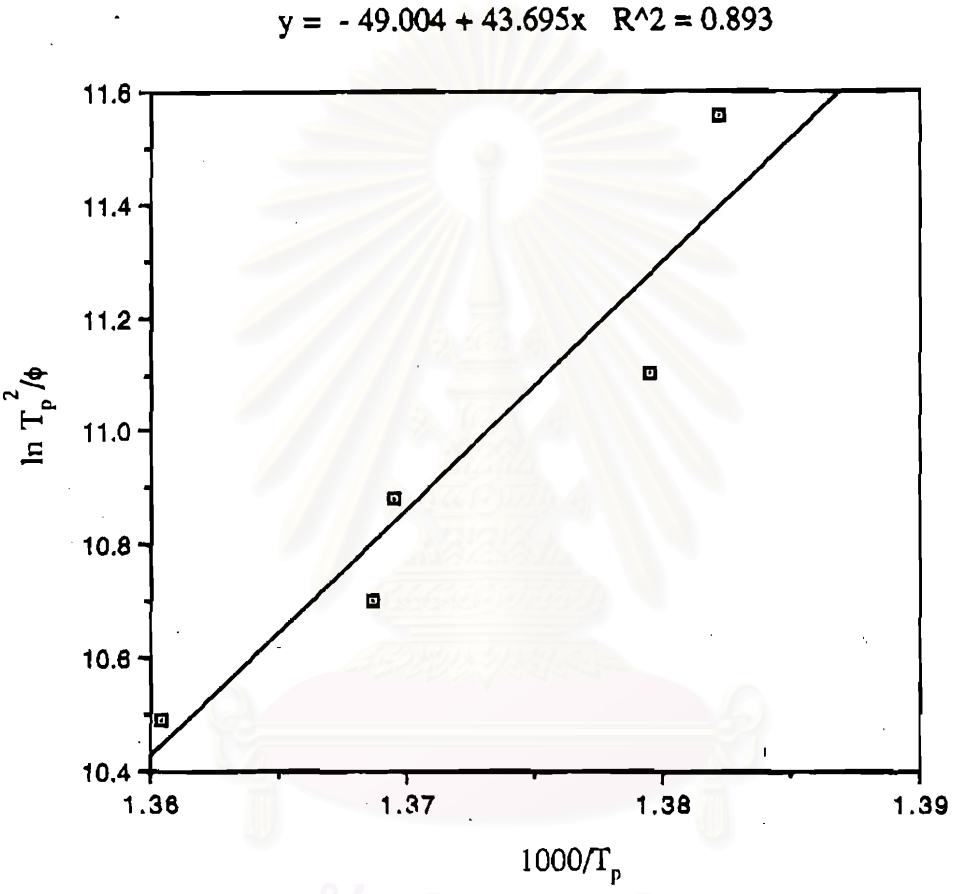

Figure 4-23 Plot of ln T_p^2/ϕ and $1000/T_p$ of CPG1 glass sample.

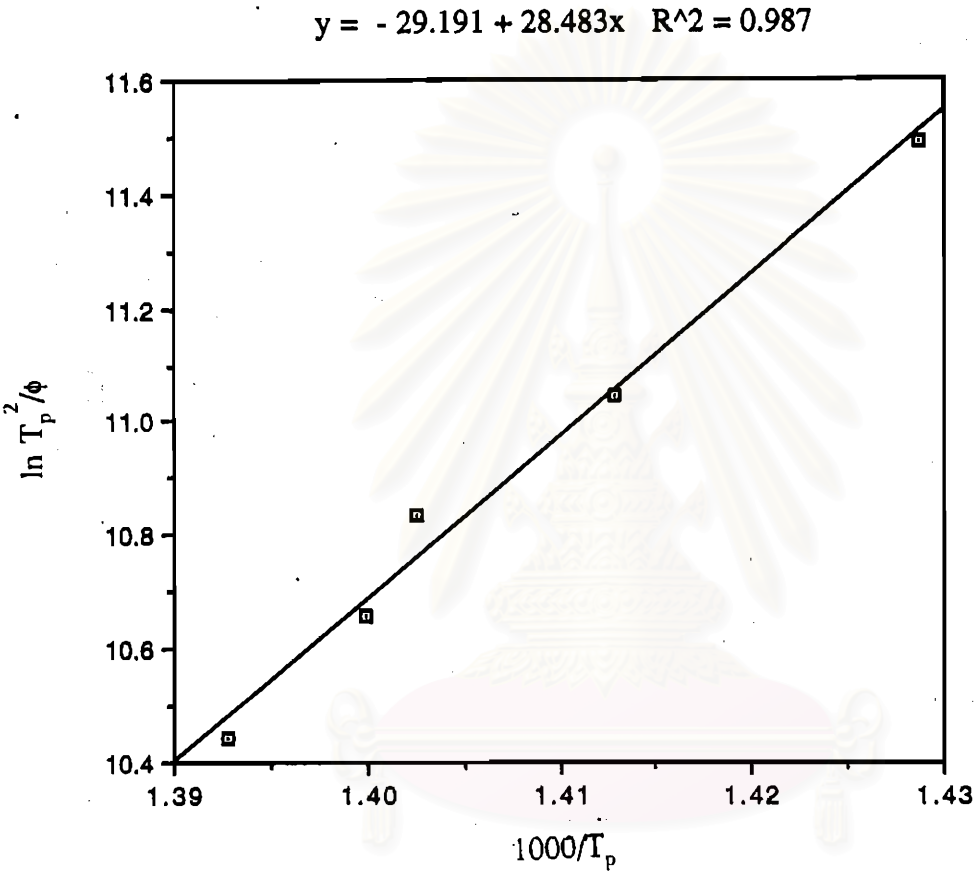

Figure 4-24 Plot of ln T_p^2/ϕ and $1000/T_p$ of CPG2 glass sample.

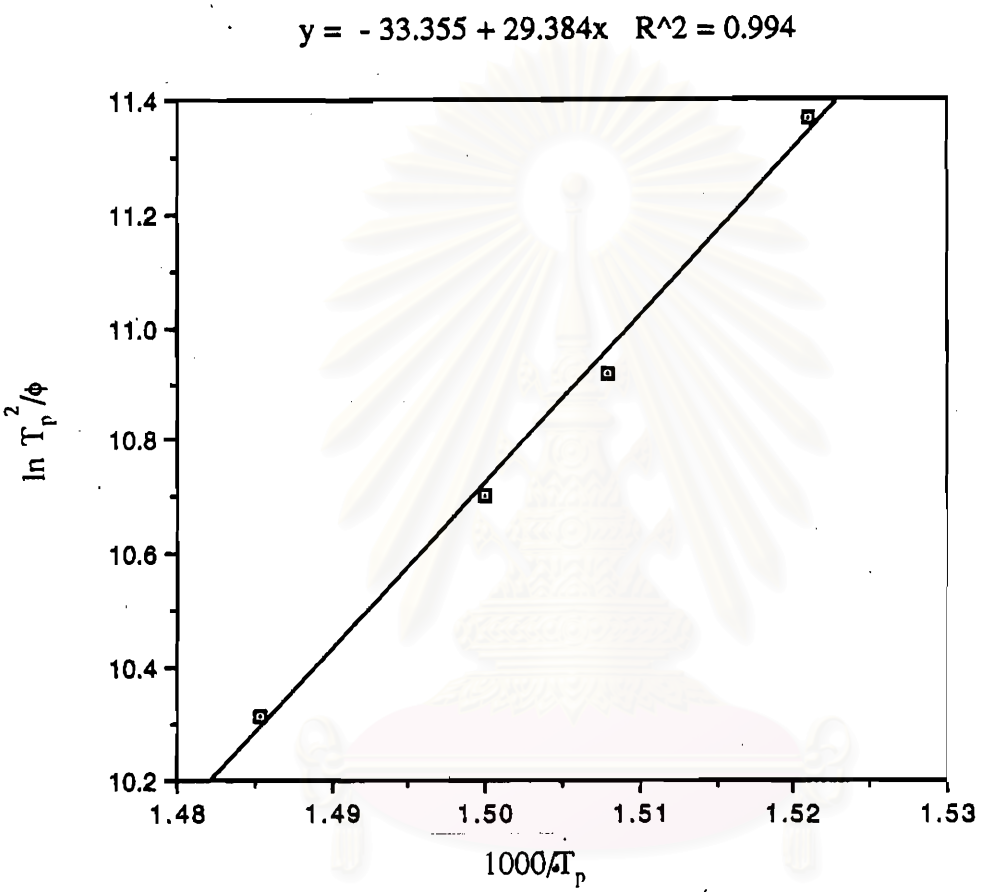

Figure 4-25 Plot of ln T_p^2/ϕ and $1000/T_p$ of CPG3 glass sample.

The shape of DTA crystallization exothermic peak could indicate the types of crystallization, i.e., a broad crystallization peak indicated a surface crystallization, whereas a sharp crystallization peak signified a bulk crystallization. The DTA crystallization exothermic peak of CPG and CPG3 glass samples showed the shape peak which was indicated that it was a bulk crystallization. In addition, CPG1 and CPG2 showed the broad peak which was indicated a surface crystallization. Moreover, Avrami parameter could be used to indicate the mechnism of crystallization, generally $n = 1$ expressed as the surface crystallization and $n = 3$ as the bulk crystallization. From the calculation of n parameter, CPG glass sample expressed $n = 29.0$ which could not be indicate the mechanism of crystallization by using Avrami parameter. CPG1, had $n = 0.94$ which could be indicated that it was a surface crystallization, CPG2 had $n = 1.5$ and could be indicated that it was a surface crystallization along with a bulk crystallization, finally CPG3 had $n = 4.0$ and could be indicated that it was a bulk crystallization. These n parameters were agreement with the shape of exothermic crystallization peak.

The activation energy of crystallization of glass samples indicated the kinetics of crystallization. If the activation energy of crystallization had a low value, the crystal could occur easily in the glass. The activation energy of crystallization of glass samples increased in the following order, CPG1 > CPG3 > CPG2 > CPG.

Abe[24] determined the activation energy of crystallization of calcium metaphosphate by Arrhenius plot, he found that the activation energy

of crystallization below T_g was 30 kcal/mol and the activation energy of crystallization above T_g was 110 kcal/mol . In this experiment the activation energy of crystallization of calcium metaphosphate (CPG) was 28.16 kcal/mol .

4.3.3 Morphology

The morphology of each CPG, CPG1, CPG2, and CPG3 glass samples which was heated isothermally at the maximum nucleation temperature for 10 min, 30 min, 2 h, 5 h, 10 h, and 24 h; it showed the extent of nuclei which increased with the time. The morphology of glass samples were illustrated in Figures 4-26, 4-27, 4-28, and 4-29, respectively. Moreover, the crystals could occur on the glass surface as the surface crystallization which could see after a long isothermal time and the crystallization was toward insides. The crystal growth began with the columnar growth and needle growth. The occurred crystal was the dendrite crystal as shown in Figure 4-30. Thus it could be referred that the nucleation rate overlapped with the crystal growth rate, because the crystallization could occur during the nucleation range.

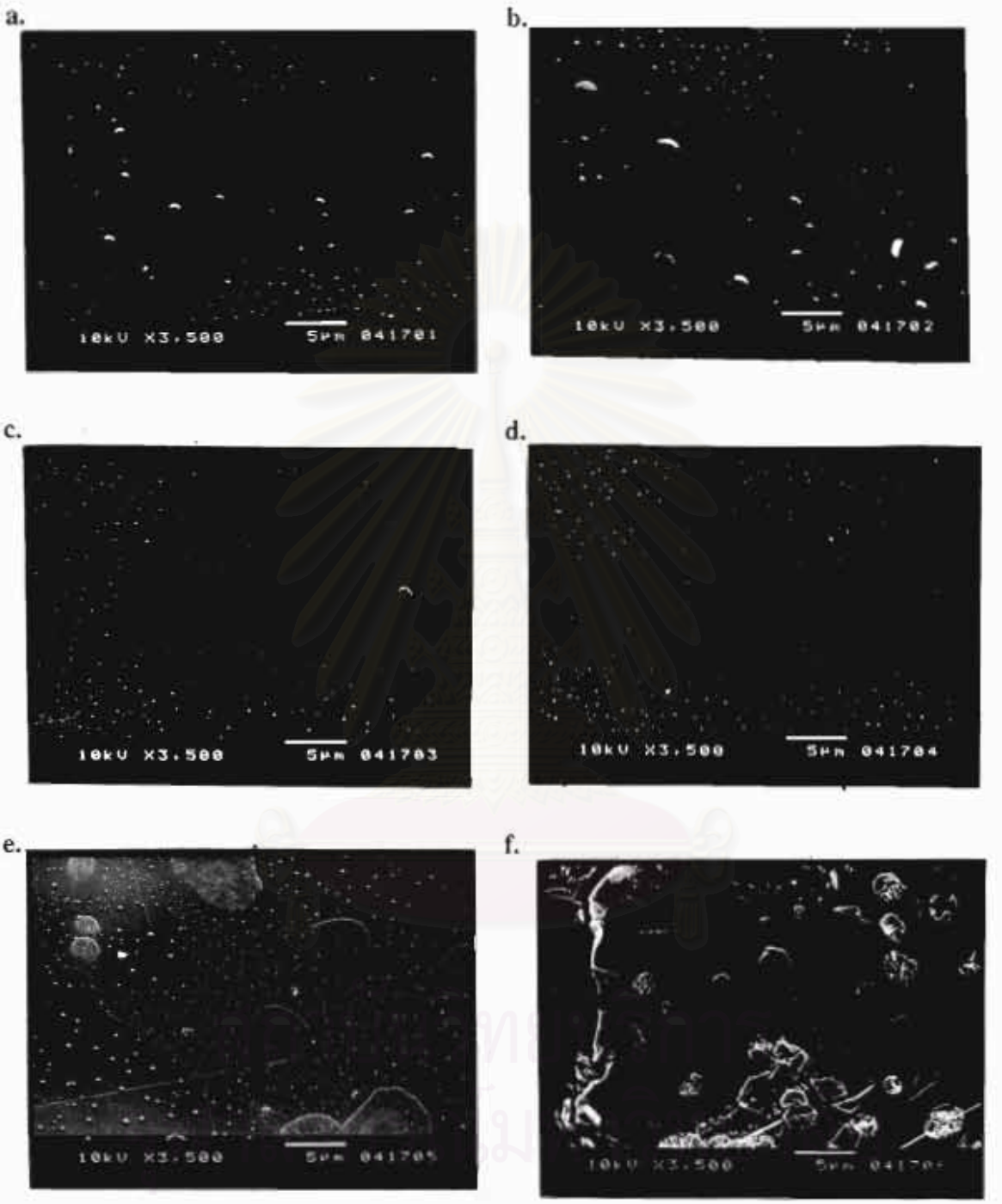

Figure 4-26 The morphology of CPG glass samples at the maximum nucleation temperature (487 °C) for a) 10 min, b) 30 min, c) 2 h, d) 5 h, e) 10h, and f) 24 h.

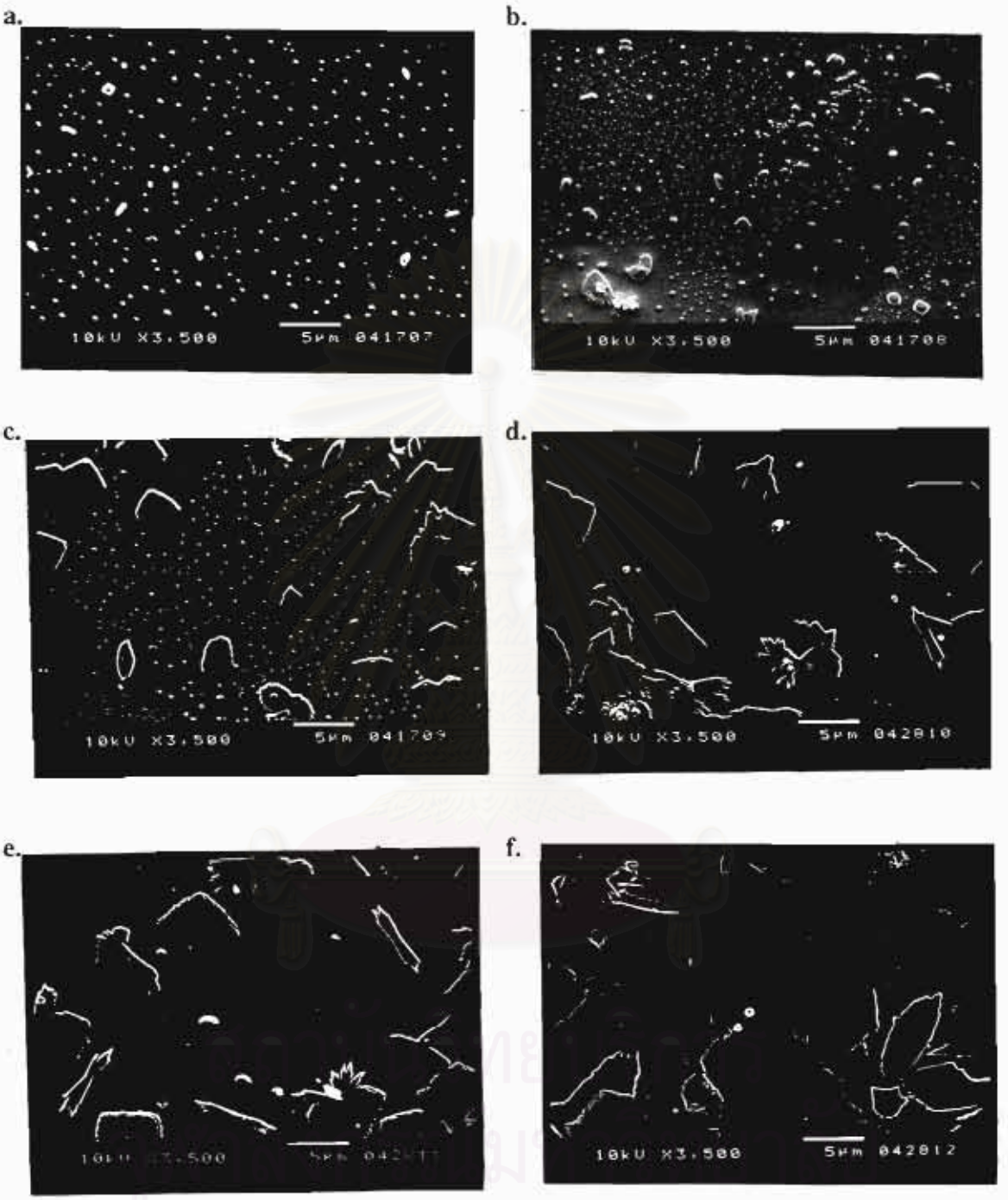

Figure 4-27 The morphology of CPG1 glass samples at the maximum nucleation temperature (569 °C) for a) 10 min, b) 30 min, c) 2 h, d) 5 h, e) 10h, and f) 24 h.

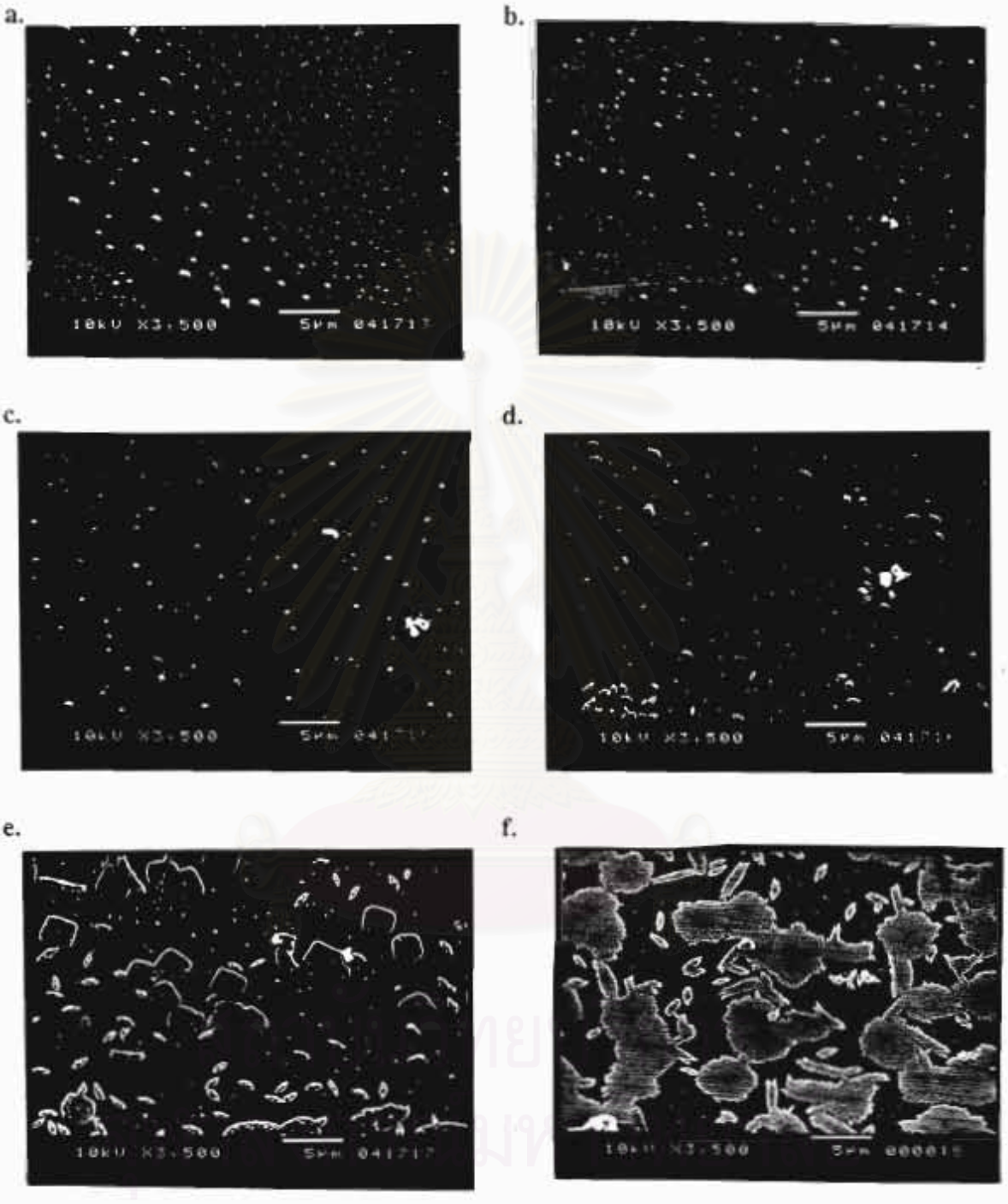

Figure 4-28 The morphology of CPG2 glass samples at the maximum nucleation temperature (559 ^{o}C) for a) 10 min, b) 30 min, c) 2 h, d) 5 h, e) 10 h, and f) 24 h

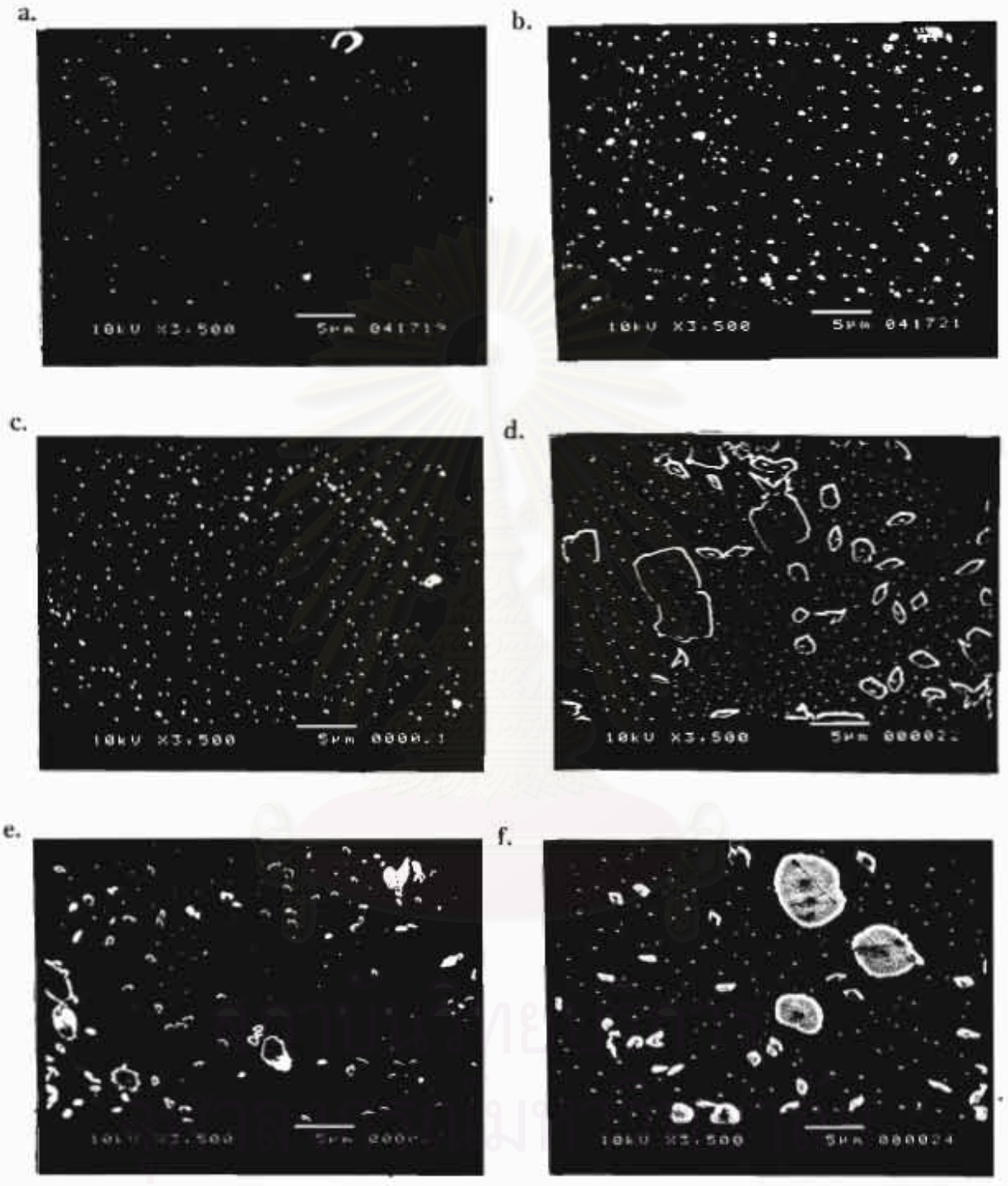

Figure 4-29 The morphology of CPG3 glass samples at the maximum nucleation temperature (579 °C) for a) 10 min, b) 30 min, c) 2 h, d) 5 h, e) 10h, and f) 24 h

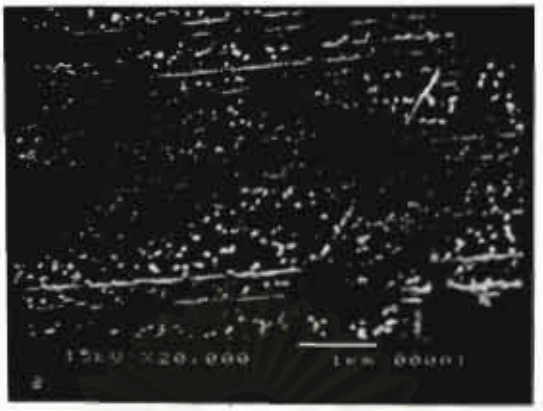

Figure 4-30 The morphology of dendrite crystal.

4.3.4 Phase identification

The crystallizations at the different temperatures of CPG, CPG1, CPG2, and CPG3 glass were analyzed and showed in Figure 4-31, 4-32, 4-33, and 4-34, respectively.

From the XRD patterns, there was a metaphase of CaP_2O_6 which occurred at below 700 ^{o}C. Its structure was a monoclinic. When the temperature increased, the metaphase changed to be $Ca(PO_3)_2$ which its structure was tetrahedra chain of PO_4. So that it could be seen the disappearance of peak patterns of CaP_2O_6. The metaphase was also shown in the DTA crystallization exothermic peak by showing the two crystallization exothermic peaks and small peaks was at below 700 ^{o}C. The interest was to find that this might result from an influence of the impurities. Both the results of DTA and XRD indicated the glass samples with high impurities would show the high amount of metaphase.

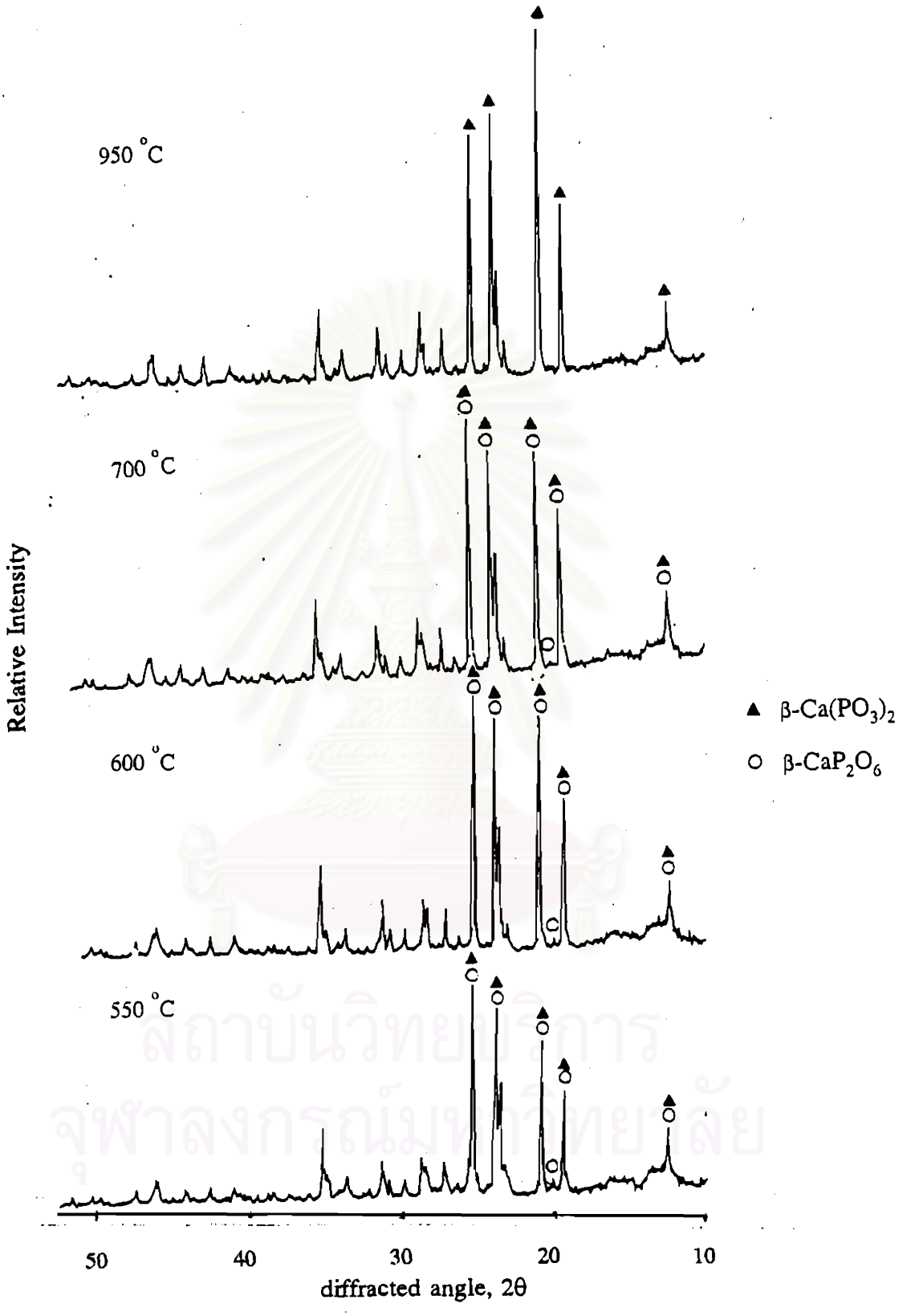

Figure 4-31 XRD patterns of CPG glass sample at the temperature between 550 ° - 900 °C.

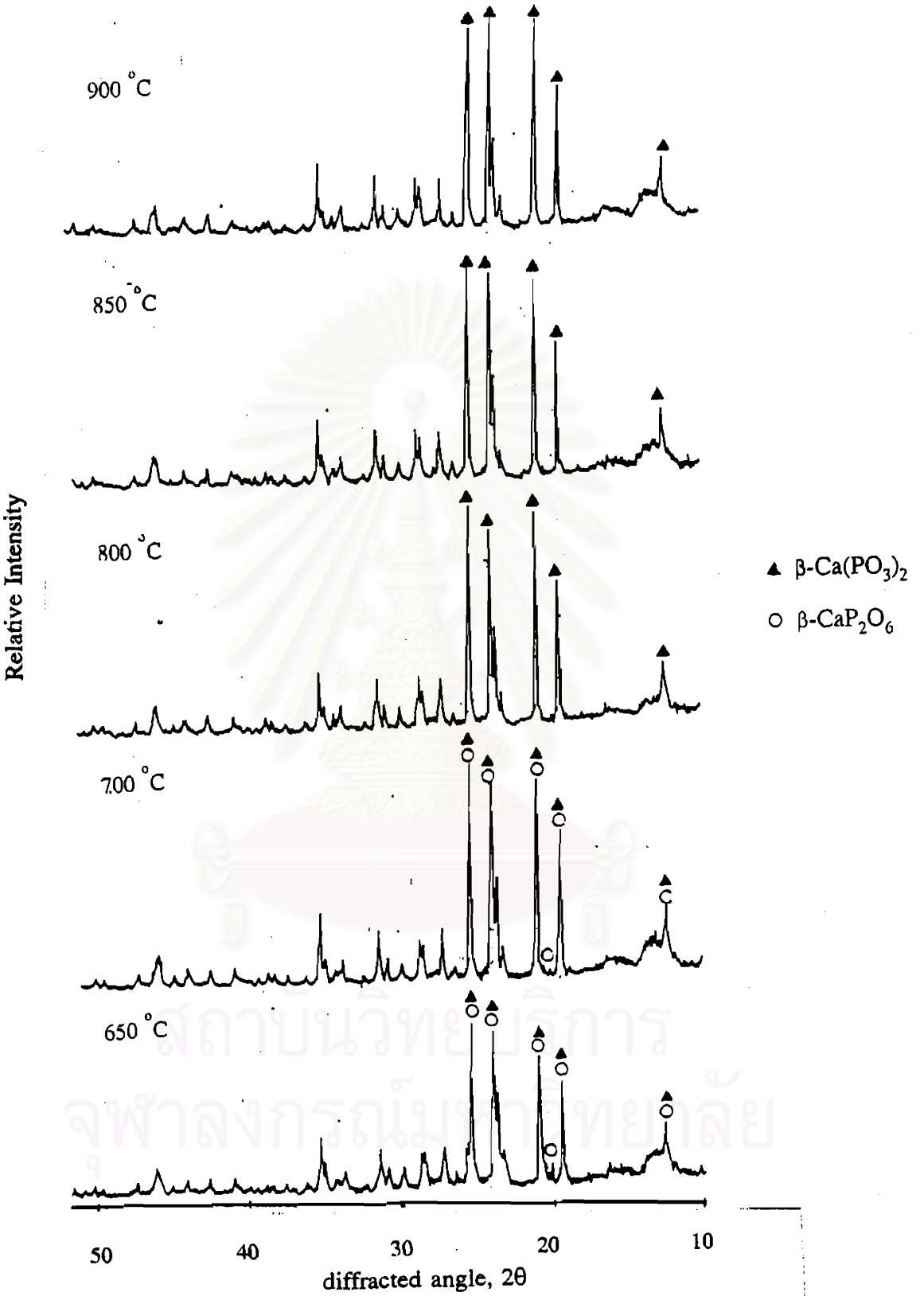

Figure 4-32 XRD patterns of CPG1 glass sample at the temperature between 650 ° - 900 °C.

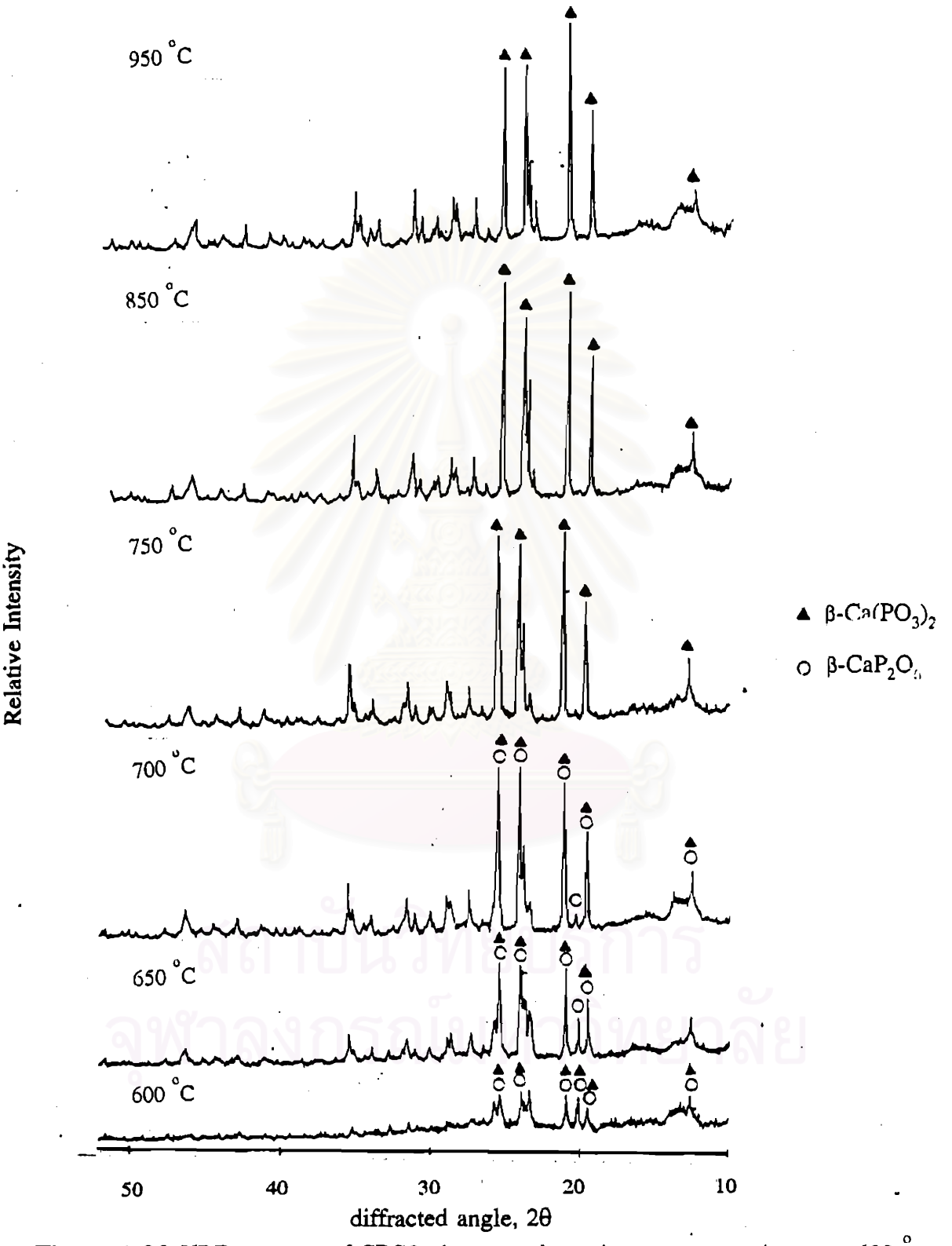

Figure 4-33 XRD patterns of CPG2 glass sample at the temperature between 600 °C - 950 °C.

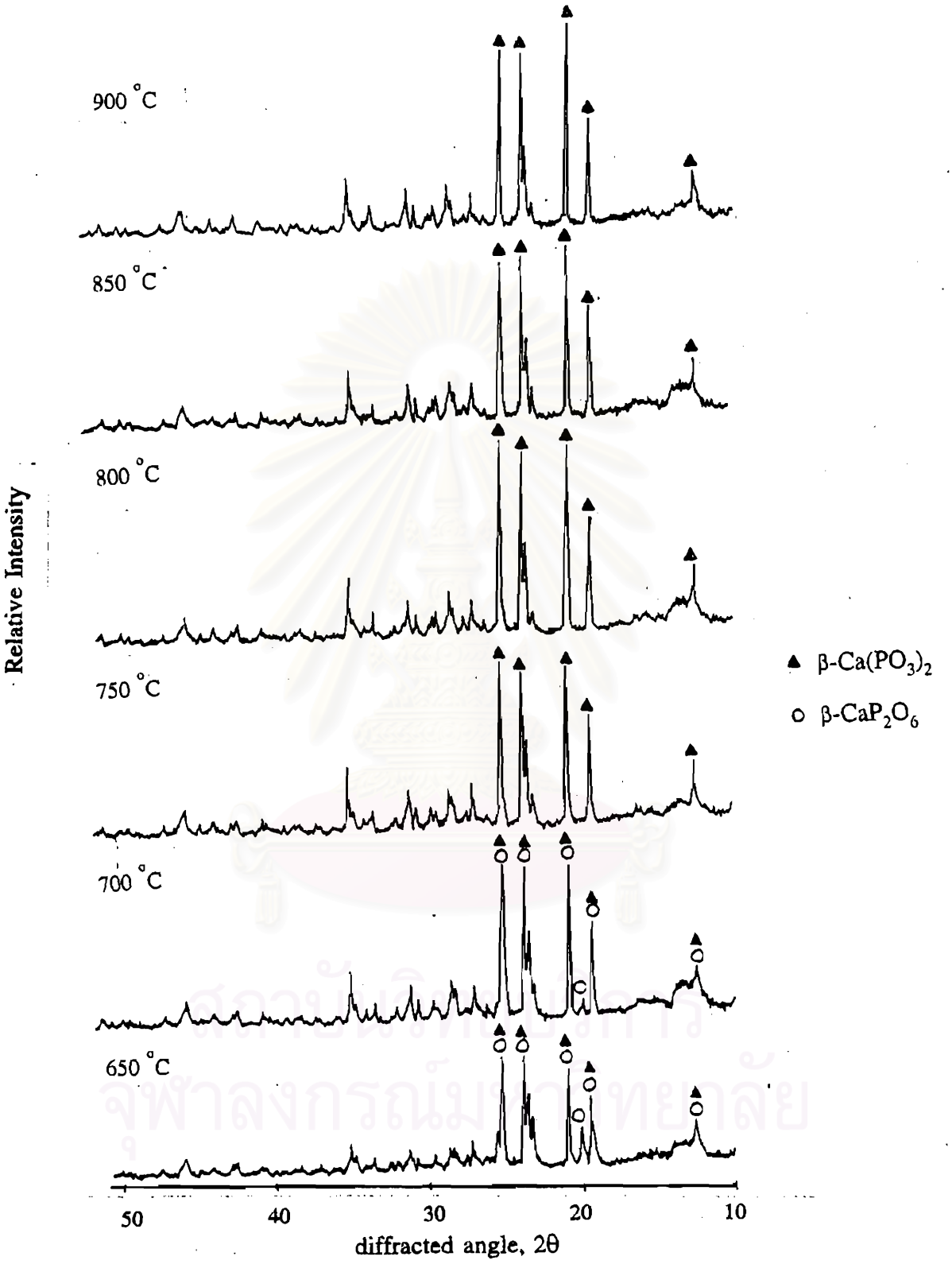

Figure 4-34 XRD patterns of CPG3 glass sample at the temperature between 650 ° - 950 °C.

4.4 Viscosity

The viscosities of CPG, CPG1, CPG2, and CPG3 glass samples were analyzed as shown in Table 4-7 and in Figure 4-35.

Table 4-7 The viscosity values of CPG, CPG1,CPG2, and CPG3 glass samples.

Glass sample	temperature (°C)	log η
CPG	1140.0	1.73
CPG1	1082.8	1.58
CPG2	1060.6	1.66
CPG3	1080.3	1.73

The viscosity was determined by drop test method, in the experiments the molten glass melted at about 1000 °C (see DTA curves in 4.2.4). In the viscosity experiments the molten glass did not fall at about 1000 °C due to the crystal occurred close to the orifice of crucible. Thus it had to increase the temperature for melting the crystal at the orifice. And the data indicated that the glass samples which gave the crystal easily or had the low activation energy of crystallization needed a higher temperature than the high activation energy of crystallization of glass samples. The comparison of JM-753 (or silicate glass) and calcium phosphate glass could be seen that by the same method the first drop of silicate glass fell at about 1200 °C which had value of log η at about 2.46, while the first drop of calcium phosphate

glass had value of log η at about 1.6 - 1.7. It could be indicated that calcium phosphate glass had a lower viscosity.

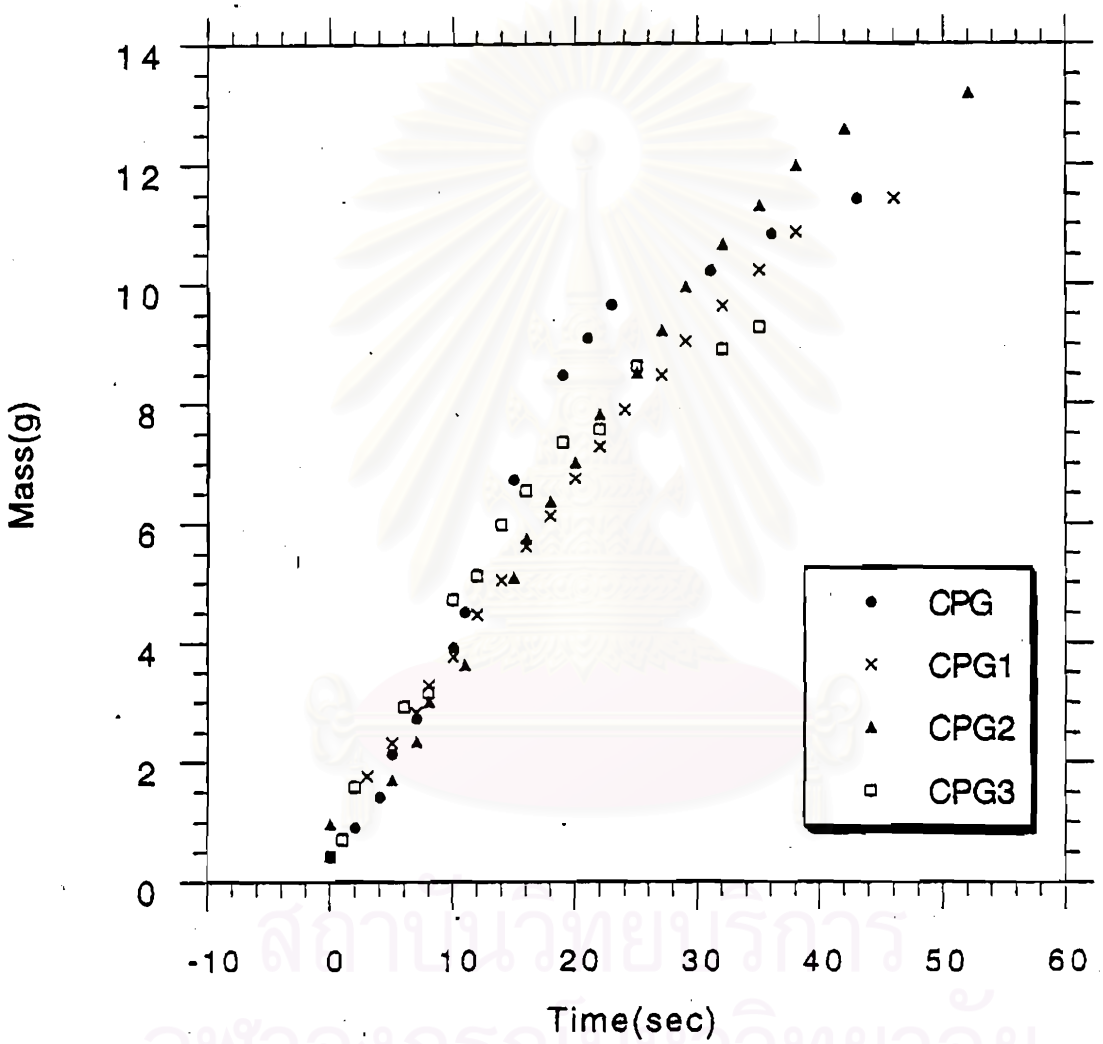

Figure 4-35 The viscosity curves of CPG, CPG1, CPG2, and CPG3 glass samples.

4.5 The glass fibers forming

There was only CPG1 could be formed the glass fibers by drawing at 1100 ^{o}C but it had a limited length (about 30 cm) and the other calcium phosphate glasses could not form the continuous glass fibers, due to at low temperature which was in the range of glass fibers formation (or at high viscosity), the crystallization occurred too fast. And at the higher temperature which had no crystallization, the viscosity was too low to form glass fibers. Generally, glass fibers could be drawn at log η = 1.5 - 3.0. The suitable condition which used to draw glass fibers depended on the viscosity; if the viscosity was much high, it could draw glass fibers easily.

The composition of glass was one of the factors which was used to consider the formation of glass fibers. In case of CPG1, there was high amount of impurities; some impurity cations could be bonded with the phosphate chain, so that these cations improved the stability of structure. In addition, CPG1 had a high activation energy of crystallization, so that the crystal occurred hardly. These helped to form glass fibers. Because the crystallization might be a cause of broken glass fibers.